



## OPEN Aridity-induced structural and functional adaptations in *Solanum surattense* across dryland ecosystems

Sadaf Rafiq<sup>1</sup>, Ummar Iqbal<sup>1</sup>, Sana Abid<sup>1</sup>, Muhammad Sharif<sup>1</sup>, Abdul Wahab<sup>1</sup>, Muhammad Kaleem<sup>2</sup>, Musarat Mansha<sup>2</sup>, Ansar Mehmood<sup>3</sup>, Shankarappa Sridhara<sup>4</sup>, Eman A. Mahmoud<sup>5</sup>, Khalid F. Almutairi<sup>6</sup>, Hosam O. Elansary<sup>6,7</sup> & Khawaja Shafique Ahmad<sup>3</sup>✉

Aridity is a key environmental filter that governs plant community structure by constraining species diversity, distribution, and adaptive capacity, particularly within arid and semi-arid ecosystems. *Solanum surattense*, a drought-resilient perennial herb, has evolved distinct morphological, anatomical, and physiological adaptations that facilitate its survival under prolonged water stress. Nevertheless, increasing anthropogenic pressure due to its high medicinal and economic value has resulted in overexploitation, leading to significant population declines and habitat fragmentation, thereby threatening its ecological sustainability and long-term persistence. This study investigates the effects of aridity on the morpho-anatomical and physiological traits of *S. surattense* populations, while also assessing its distribution across ecologically diverse habitats in Punjab, Pakistan. Ten populations of *S. surattense* were collected from ecologically distinct habitats of the Cholistan Desert and its margins to evaluate key anatomical and physiological traits contributing to its ecological success under varying aridity levels. The De Martonne aridity index<sup>1</sup> was used to assess aridity levels, with populations sampled from the Cholistan Desert (IDM = 8.96–7.21) and its margins (IDM = 17.49–14.99). Advanced microscopy techniques (rotary microtomy and stereo microscopy) were employed to analyze its morphological and physiological traits. Populations from the Cholistan Desert exhibited distinct xeromorphic adaptations to survive in hyper-arid environments. These included a significantly thickened epidermis, encrypted stomata (128.13  $\mu\text{m}^2$ ), well-developed vascular tissues, and prominent storage parenchyma in both stems and leaves. Structural reinforcements such as enhanced cortical thickness (120.33  $\mu\text{m}$ ), pith development (118.58  $\mu\text{m}$ ), and vascular bundle area (74.41  $\mu\text{m}^2$ ) contributed to improved water retention and mechanical support under drought stress. Physiologically, desert populations showed elevated levels of osmolytes—including proline (39.65  $\mu\text{mol g}^{-1}$  fw.), soluble sugars (13.39  $\mu\text{mol g}^{-1}$  fw.), and free amino acids (22.35  $\mu\text{mol g}^{-1}$  fw.)—which facilitate osmotic adjustment and cellular stabilization during dehydration. In contrast, populations from the Cholistan Desert margins displayed superior growth performance, characterized by greater shoot length (55.66 cm), larger leaf area (25.24  $\text{cm}^2$ ), higher flower (24.35 per shoot) and fruit production (23.74 per shoot), and increased shoot biomass (41.66  $\text{g plant}^{-1}$ ). These marginal populations also demonstrated improved photosynthetic capacity, indicated by higher chlorophyll a and b contents (1.62  $\text{mg g}^{-1}$  fw. and 1.24  $\text{mg g}^{-1}$  fw.), increased total chlorophyll (2.94  $\text{mg g}^{-1}$  fw.), and optimized carotenoid levels (0.30  $\text{mg g}^{-1}$  fw.), supporting greater energy capture and stress mitigation. An increased stomatal density (35.95  $/\text{mm}^2$ ), coupled with reduced midrib and lamina thickness and enlarged vascular tissues, contributed to improved resource transport and gas exchange. Collectively, the results reveal a pronounced ecological divergence between *Solanum surattense* populations inhabiting the hyper-arid core of the desert and those from its peripheral zones, indicative of an adaptive trade-off between drought resistance and growth performance. These findings underscore the species' functional plasticity and resilience, offering valuable insights into plant survival strategies under extreme climatic stress. Elucidating such intraspecific trait variability holds significant implications for restoration ecology, targeted conservation efforts, and the development of sustainable land management practices in arid and semi-arid landscapes.

**Keywords** Drought adaptation, Structural plasticity, Biochemical adaptation, Osmotic regulation, Stomatal dynamics, Conservation strategy

<sup>1</sup>Department of Botany, The Islamia University of Bahawalpur, Rahim Yar Khan Campus, Bahawalpur 64200, Pakistan. <sup>2</sup>Department of Botany, University of Agriculture Faisalabad, Faisalabad 38040, Pakistan. <sup>3</sup>Department of Botany, University of Poonch Rawalakot, Rawalakot 12350, Pakistan. <sup>4</sup>Center for Climate Resilient Agriculture, University of Agricultural and Horticultural Sciences, Shivamogga 577201, India. <sup>5</sup>Department of Food Science, College of Agriculture, Damietta University, Damietta, Egypt. <sup>6</sup>Department of Plant Production, College of Food and Agriculture Sciences, King Saud University, Riyadh 11451, Saudi Arabia. <sup>7</sup>Prince Sultan Bin Abdulaziz International Prize for Water Chair, Prince Sultan Institute for Environmental, Water and Desert Research, King Saud University, Riyadh 11451, Saudi Arabia. ✉email: ahmadks@upr.edu.pk

Aridity functions as a potent environmental filter, significantly shaping plant community composition and regulating ecosystem processes such as primary productivity and nutrient cycling<sup>1–3</sup>. In the context of climate change, which is projected to exacerbate aridity levels globally—particularly in dryland regions<sup>4</sup> substantial shifts in vegetation structure, dominant plant functional traits, and functional dispersion (FDis) are anticipated. Intensifying aridity is likely to favor specific life forms, including grasses and prostrate species, while selecting for smaller plants that reduce hydraulic vulnerability, and promote early flowering and shorter reproductive periods<sup>5</sup>. Dispersal strategies may also shift, with greater seed mass and longevity offering a competitive advantage under episodic resource availability. Belowground trait diversification, particularly in root morphology, may enhance water and nutrient uptake during resource pulses. Moreover, plant communities may become increasingly dominated by stress-tolerant taxa characterized by evergreen foliage and low specific leaf area (SLA). However, shifts in trait dominance and FD can influence ecosystem functioning and resilience, as higher FDis is associated with enhanced ecosystem processes and greater adaptability to arid conditions<sup>6</sup>.

Aridity is a dominant abiotic driver shaping structure and functioning of grassland ecosystems, particularly across broad spatial gradients where water availability is a primary limiting factor<sup>7</sup>. The projected increase in aridity is expected to diminish the capacity of global grasslands to sustain essential ecosystem services<sup>8</sup>. Empirical evidence indicates that aridity reduces plant species richness and productivity while modifying the composition and structure of both aboveground and belowground biotic communities at local, regional and global scales<sup>9</sup>. Given that fundamental ecosystem processes, such as nitrogen cycling, carbon sequestration, and litter decomposition are regulated by these biotic components, they are likely to decline in response to increasing aridity<sup>10,11</sup>. Furthermore, the ecological responses of grasslands to climate change are modulated by land-use practices<sup>12</sup> however, the interactive effects of land use and aridity on ecosystem functioning, particularly through potential shifts in biodiversity, remain poorly understood at large spatial scales.

Aridity plays a complex role in shaping composition and diversity of plant communities in dryland ecosystems<sup>13</sup>. Emerging evidence indicates that facilitative interactions among plant species may intensify moderate aridity, potentially mitigating the negative effects of climate change on plant diversity<sup>14</sup>. However, under extreme aridity, facilitation may deteriorate, accelerating climate-driven decline in plant richness<sup>15</sup>. Both competitive and facilitative dynamics are known to operate across environmental gradients, with the nature of resource competition shifting from above-ground to below-ground as conditions become more arid<sup>14,16</sup>. In parallel, global climate change is contributing to extensive tree mortality even within mesic habitats<sup>17</sup> a phenomenon increasingly linked to the combined effects of heat and drought stress<sup>18</sup>. Plant adaptation to drought involves trade-offs between stomatal traits, which regulate water loss and CO<sub>2</sub> uptake, and hydraulic traits that sustain water transport and prevent embolism<sup>19,20</sup>. Together, these functional traits encompass a continuum of morphological and physiological strategies that underlie plant resilience across a broad range of climatic regimes<sup>21</sup>.

*Solanum surattense* Burm.f. is a perennial wild herb belonging to family Solanaceae, extensively employed in traditional and folk medicine across tropical and subtropical regions of Southeast Asia, with a notable prevalence in Pakistan. It is characterized by the presence of prickles on its leaves and stems. This species exhibits polymorphism, with purple flowers being the most common, though white-flowered variants are occasionally observed<sup>22,23</sup>. *S. surattense* is a prickly, diffuse herb with procumbent branches densely covered in bright yellow prickles. Its leaves are deeply pinnately lobed, highly spiny, and have a sinuous outline with an asymmetrical base. The flowers are pentamerous, varying in color from purple to bluish-purple. The fruit is a spherical berry, initially white with green markings when immature, turning light yellow or whitish upon ripening. *S. surattense* typically inhabits dry, open environments such as roadsides, wastelands, and degraded forest margins, demonstrating a high degree of xerophytic adaptation. Phytochemical investigations have revealed a diverse array of bioactive compounds, including alkaloids, flavonoids, phenols, and steroids<sup>24</sup>. Traditionally, the species is valued for its anti-inflammatory, analgesic, and cardiac agents, and is widely used to treat coughs and various skin disorders<sup>25</sup>.

*Solanum surattense* is widely distributed across the Cholistan Desert and its marginal areas of Punjab, Pakistan, playing a crucial role in supporting local wildlife and offering significant ethno-medicinal value. However, excessive exploitation for medicinal and economic purposes has raised serious concerns about habitat degradation and species sustainability<sup>24,25</sup>. Overharvesting, coupled with increasing aridity and anthropogenic pressures, have contributed to habitat fragmentation and population decline, posing a substantial threat to its long-term survival. This study provides the first report on its partial distribution across arid regions, emphasizing the combined influence of environmental stressors and human disturbances on its ecological range. Understanding these dynamics is essential for developing conservation strategies to mitigate habitat loss and ensure the persistence of this ecologically and medicinally valuable species. This study aims to identify plant functional traits responding to aridity in the Cholistan Desert and its adjacent regions by analyzing the

functional structure and growth behavior of plant populations along a spatial aridity gradient using the De Martonne Aridity Index<sup>1</sup> as adapted by Baltas<sup>26</sup>. We hypothesize that aridity functions as a key environmental filter, shaping species traits from the regional species pool. Specifically, we predict that (i) increasing aridity will alter the functional structure of *S. surattense* populations, and (ii) populations exposed to higher aridity will exhibit traits associated with drought resistance and climatic adaptability, consistent with ecological filtering in dryland systems.

Materials and methods  
Study area and sampling design

The study was conducted in an arid to semi-arid climate of Punjab, Pakistan, characterized by an average annual precipitation of approximately 200 mm over the past decade. The region experiences extreme temperature variations, with average summer highs ranging from 36 °C to 48 °C in June, while winter lows drop to approximately 6.67 °C in January. The driest months, May to June, receive around 150 mm of rainfall, whereas the wetter months, from October to January, see precipitation levels of approximately 200 mm.

Plant samples were collected during the spring of 2023, ensuring that the study focused on mature plants under relatively stable climatic conditions before the onset of the wet season. Ten distinct populations of *S. surattense* were collected from ecologically diverse regions of Punjab, Pakistan, to investigate population variability under varying ecological conditions (Table 1; Fig. 1). These included: (i) Cholistan Desert—sand dunes in Rahim Yar Khan, desert canal in Baghu Bahar, desert flats in Aman Garh, saline desert in Sardar Garh, and mud flats in Fatehpur Kamal; (ii) Cholistan Desert margins—roadside in Thull Hamza, agricultural land in Uch Sharif, wasteland in Khanpur, barren land in Kot Mithan, and salt-affected land in Basti Zahir Peer. Plant and soil samples were systematically collected from each site, ensuring the inclusion of both plant physical characteristics and rhizospheric soil for habitat-specific adaptation analysis. Samples were randomly selected, labeled, and preserved for laboratory analysis, with soil samples specifically assessed for pH, salinity, organic matter, and essential nutrient composition. Plant material (*S. surattense*) was collected from the Cholistan region, Pakistan, with prior permission obtained from the Punjab Forest, Wildlife & Fisheries Department (Permit No. FWFP-216). A voucher specimen was deposited in [Poonch Herbarium, Accession No. POONCH-1802], and species identification was confirmed by Dr. Sajjad Hussain, Curator, Poonch Herbarium, Department of Botany, University of Poonch Rawalakot.

Seasonal variations in rainfall and temperature were accounted for by integrating meteorological data from each district, obtained from the respective meteorological department. This dataset included temperature, humidity, and precipitation records, ensuring that sampling was conducted under representative climatic conditions. Additionally, geospatial accuracy was maintained by using a Global Positioning System (GPS) to record precise coordinates and altitude for each sampling site. This approach enabled a comprehensive analysis of how climatic fluctuations influenced plant functional traits and soil properties.

Plant and soil sampling randomization

At each study site, a 50×50 m plot was established, and a randomized grid sampling method was used to select individual plants. Within each plot, five quadrats measuring 5×5 m were randomly designated. From each quadrat, ten mature individuals of *S. surattense* were selected, randomly, yielding a total of 50 plants per site. The criteria for plant selection included morphological traits such as plant height, branching pattern, and the number of flowers and fruits per plant to ensure representative sampling of the population. To analyze soil characteristics, three composite soil samples were collected from randomly selected points within each quadrat. Sampling was conducted at a depth of 0–30 cm to capture the root zone environment. A transect-based randomization approach was applied, where soil cores were taken at five equidistant points per transect and mixed to form a composite sample. This ensured that the collected soil adequately represented the heterogeneity within each study site.

Ecological regions	Sites	Habitat types	Soil texture	Maximum temperature (°C)	Minimum temperature (°C)	Relative humidity (%)	Rainfall (mm)	IDM
Cholistan Desert	Rahim Yar Khan	Sand dunes	Sandy loam	48.23a	12.60a	21.85e	101.36f	8.91e
	Bagho Bahar	Desert canal	Loamy	44.13d	12.12b	20.90f	98.20 g	8.96e
	Aman Garh	Desert flats	Loamy sand	46.13b	10.46c	19.40 g	116.24e	8.61f
	Sardar Garh	Saline desert	Sandy loam	43.13e	9.15f	17.91 h	113.21e	8.00 g
	Fateh Pur Kamal	Mud flats	Clay loam	45.13c	9.35ef	22.39e	108.14f	7.21 h
Cholistan Desert Margins	Thull Hamza	Roadside	Clayey loam	40.50 g	9.13 g	40.30a	137.08de	17.49a
	Uch Sharif	Agriculture land	Clayey loam	42.75f	7.13j	39.55ab	160.48a	16.02b
	Khan Pur	Wasteland	Loamy	43.88e	8.13i	37.31b	138.32d	15.90c
	Kot Mithan	Barren land	Clay loam	43.88e	8.47 h	35.60c	146.82c	14.99d
	Bait Zahir Pir	Salt-affected land	Loamy	45.00c	9.47de	30.15d	156.82ab	14.99d

**Table 1.** Topographic and relief factors of *Solanum surattense* along with types of Climatic zones according to the de Martonne aridity index (IDM arid < 10.0; Semi-arid < 20.0), adapted after Baltas (2007).



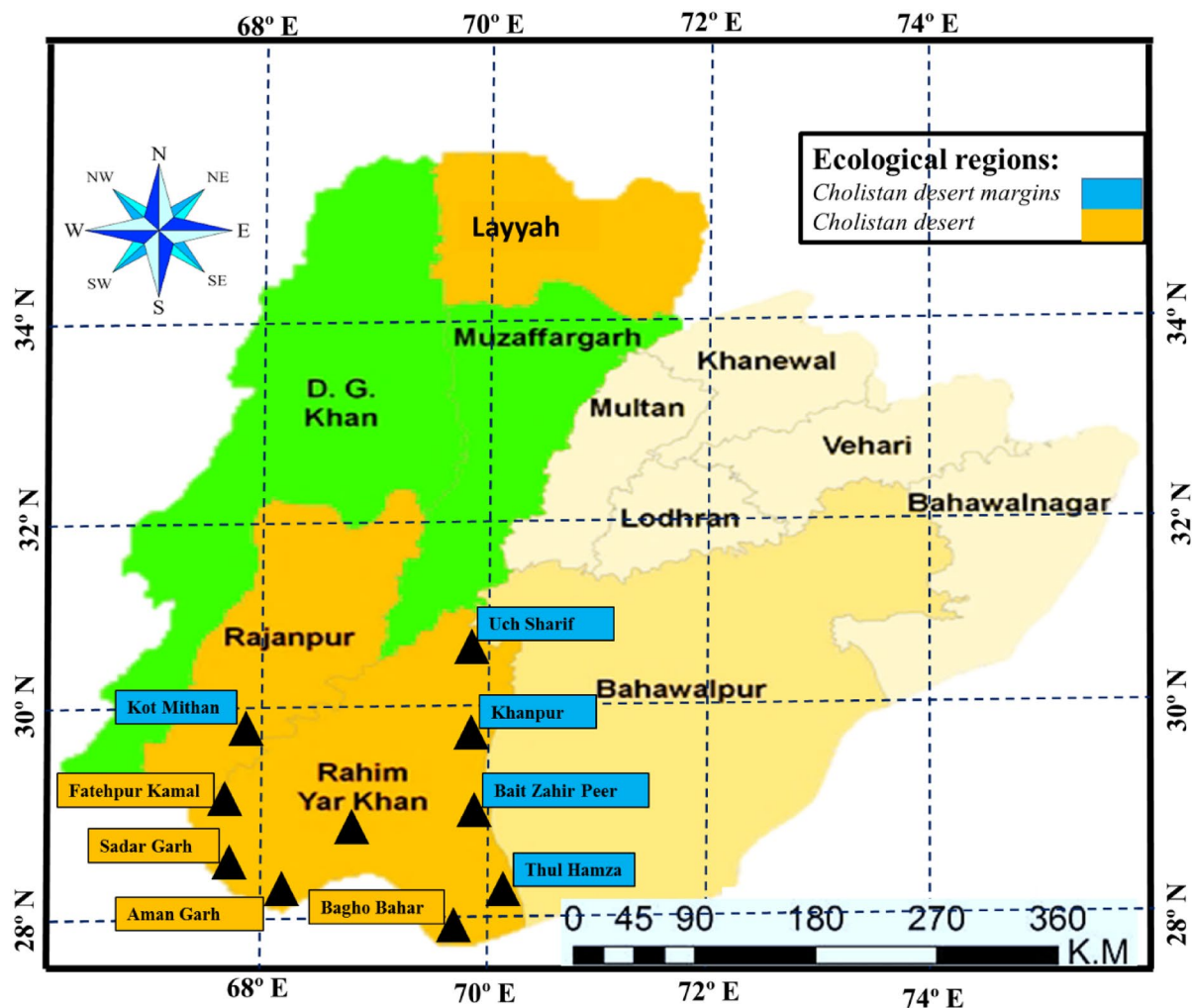


**Fig. 1.** Punjab map showing collection sites and panoramic view of *Solanum surattense* sampled from different ecological regions. Different locations within these regions are marked with colored triangles representing abundance levels. The Cholistan Desert Margins are shown in blue, while the Cholistan Desert is depicted in orange. Map created using the ggspatial package in R-Studio in R program with geographical data sourced from ArcGIS Pro (Ver.10.8). Projection system: [UTM Zone 42 N]. Boundary and terrain information were adapted from available GIS datasets.



De Martonne aridity index calculation

The De Martonne Aridity Index was chosen over other aridity metrics due to its simplicity, broad applicability, and ability to scales effectively. Unlike other indices that require complex datasets or multiple climate variables, the IDM relies on two fundamental and widely available parameters: precipitation and temperature. This makes it particularly useful for assessing aridity in regions with limited meteorological data, such as the Cholistan Desert. The IDM was formulated by Emmanuel de Martonne in the early 20th century to assess climate dryness or aridity (Table 1). It was calculated annually or at more frequent intervals to evaluate whether a region's climate was arid or humid. According to the IDM, a climate was classified as arid when the IDM was below 10.0 and semi-arid when it was below 20.0<sup>26</sup>.

<sup>11</sup>The index is computed using the following formula:

$$\text{De Martonne Aridity Index (IDM)} = \frac{P}{Ta + 10}$$

Where:

P represents the annual precipitation (in millimeters).

T<sub>a</sub> represents the mean annual temperature (in degrees Celsius).

The constant 10 is added to the temperature to avoid negative values and account for the variability of aridity in different climatic zones.

Soil parameters

Fresh soil samples were weighed using a digital balance and oven-dried at 70 °C until a constant weight was achieved (Table 2). Soil moisture content was calculated as the difference between fresh and dry weights. Further, a soil saturation paste was prepared, and soil water was extracted using a vacuum pump. Soil electrical conductivity (ECe) and pH were measured using an ECe/pH meter (Ino LAB pH/Cond 720, WTW series). The concentrations of sodium (Na<sup>+</sup>), potassium (K<sup>+</sup>), and calcium (Ca<sup>2+</sup>) ions were determined using a flame photometer (PFP-7, Jenway, Staffordshire, UK). Phosphate (PO<sub>4</sub><sup>3-</sup>) concentrations were quantified spectrophotometrically following the method of Yoshida<sup>27</sup> while nitrate (NO<sub>3</sub><sup>-</sup>) levels were measured according to the procedure described by Kowalenko<sup>28</sup>. The soil saturation percentage was determined using the method outlined by Richards<sup>29</sup> and organic matter content was assessed following the procedure described by Sims and Haby<sup>30</sup>.

Plant analysis

Growth parameters

Plants were carefully uprooted using a plant auger (20 cm diameter) to minimize root damage and then gently washed in a water cooler. Fresh weights of the roots and shoots were immediately recorded using a portable digital balance. The dry weights were later measured in the laboratory after drying the plant material for one week at 60 °C. The lengths of roots, shoots, and inflorescences were measured using a standard measuring

Ecological regions	Sites	Habitat types	pH	ECe (dS/m)	Na <sup>+</sup> (mg kg <sup>-1</sup> )	K <sup>+</sup> (mg kg <sup>-1</sup> )	Ca <sup>2+</sup> (mg kg <sup>-1</sup> )	OM (%)	SP (%)	NO <sub>3</sub> <sup>-</sup> (mg kg <sup>-1</sup> )	PO <sub>4</sub> <sup>3-</sup> (mg kg <sup>-1</sup> )
Cholistan Desert	Rahim Yar Khan	Sand dunes	7.02±0.08a	0.75±0.05 h	85.76±6.21 h	63.29±4.17f	66.32±3.94 g	0.15±0.01 g	11.32±0.9f	1.27±0.14e	1.09±0.12j
	Bagho Bahar	Desert canal	6.94±0.07b	0.83±0.06 g	98.53±7.13 g	116.31±5.87d	79.74±4.11f	0.39±0.02c	22.53±0.8 cd	2.74±0.16bc	1.39±0.11 g
	Aman Garh	Desert flats	7.02±0.08a	0.93±0.07f	47.62±3.89i	76.31±9.23e	52.24±3.79 h	0.22±0.01f	19.76±1.7d	3.13±0.18c	2.66±0.15c
	Sardar Garh	Saline desert	6.77±0.06c	4.60±0.04c	398.45±3.14c	44.91±4.02i	42.45±2.97j	0.23±0.02f	12.53±0.8ef	2.27±0.14d	1.15±0.10i
	Fateh Pur Kamal	Mud flats	6.77±0.06c	0.60±0.0i	42.45±3.14j	54.91±4.02 g	57.45±2.97i	0.33±0.02e	12.53±0.8ef	2.27±0.14d	1.25±0.10 h
Cholistan desert Margins	Thull Hamza	Roadside	6.45±0.05d	2.71±0.15d	232.70±9.32e	141.69±7.43c	176.21±5.49b	0.57±0.02b	21.75±0.7c	2.51±0.13c	1.72±0.14e
	Uch Sharif	Agriculture land	5.00±0.04e	1.27±0.22e	112.44±11.27f	190.44±3.67b	222.27±7.94a	0.87±0.02a	28.20±1.5a	3.58±0.14a	2.83±0.13a
	Khan Pur	Wasteland	7.10±0.09a	5.24±0.21b	392.70±12.36d	203.88±9.46a	153.03±4.02c	0.42±0.01c	24.76±1.7b	3.13±0.18b	2.66±0.15b
	Kot Mithan	Barren land	5.00±0.04e	5.27±0.22b	412.44±11.27b	50.44±3.67 h	122.27±7.94d	0.37±0.02d	21.20±1.5 cd	2.58±0.14c	2.43±0.13d
	Bait Zahir Pir	Salt-affected land	6.61±0.06 cd	6.04±0.24a	584.96±14.52a	82.74±4.82de	86.86±6.32e	0.22±0.01a	13.32±0.9e	1.57±0.10a	1.49±0.12f

**Table 2.** Soil parameters of *Solanum surattense* sampled from dryland ecosystems. Values are mean ± se (n = 10). Mean values in a column with different superscript letters are significantly different (p < 0.05 of the analysis of variance –ANOVA-across sites and post-hoc least significant difference –LSD-test of multiple comparisons among sites).

scale. Other morphological traits, including the number of leaves, fruits, flowers, and thorns per branch, were manually counted. Leaf area was determined using a formula developed by Schrader et al. (2021).

$$\text{Leaf area} = \text{Length} \times \text{Width} \times \text{Correction factor (0.69)}.$$

#### *Physiological parameters*

Fresh plant samples were stored in Falcon® tubes at  $-80^{\circ}\text{C}$  for subsequent chlorophyll pigment and osmolyte analysis. Proline content was measured using the Bates method<sup>31</sup> in which fresh leaves were ground in potassium phosphate buffer (pH 7.8), centrifuged, and analyzed by measuring absorbance at 595 nm. Total free amino acids were assessed using the Moore and Stein<sup>32</sup> method, where leaves were extracted in citrate buffer (pH 5.0), heated with ninhydrin, and absorbance was recorded at 530 nm. Total soluble sugars were determined following a modified Yemm and Willis<sup>33</sup> method. In this process, leaves were homogenized in chilled ethanol, centrifuged, reacted with anthrone reagent, and absorbance was measured at 620 nm. Photosynthetic pigments, including chlorophyll *a*, chlorophyll *b*, total chlorophyll, and carotenoids, were quantified using a spectrophotometer (Hitachi-220, Japan) following the methods of Arnon and Davis<sup>34</sup>.

#### *Anatomical parameters*

To examine the anatomical characteristics, small sections ( $\sim 2$  cm each) were excised from specific plant parts, including the topmost internode of the stem, the root-shoot junction, and the basal portion of the corresponding leaf. The collected samples were initially preserved in formalin-acetic-alcohol (FAA) solution (5% formalin, 50% ethyl alcohol, 10% acetic acid, and 35% distilled water) to maintain tissue integrity. For long-term preservation, the material was subsequently transferred to a solution of 75% ethyl alcohol and 25% acetic acid to ensure optimal sample stability. For detailed anatomical analysis, a rotary microtome was used to obtain precise, thin sections of the preserved tissues, enabling the production of fine, uniform slices essential for clear microscopic examination. The tissue sections were then stained, mounted on slides, and observed under a microscope. Final images were captured using stereo microscopy (Nikon SE, Anti-Mould, Tokyo, Japan), providing high-resolution views of the cellular and structural features of each plant part. This methodology ensured a rigorous and accurate analysis of the anatomical characteristics.

#### **Computational analysis**

Statistical analysis was performed using one-way Analysis of Variance (ANOVA) based on a completely randomized design with ten replications. An F-test was conducted to assess the significance of various variables, followed by a Least Significant Difference (LSD) test to compare means ( $P > 0.05$ ) using Minitab (Minitab, LLC, State College, PA, USA). Multivariate statistical analyses, including Principal Component Analysis (PCA), were utilized to assess the influence of soil physicochemical properties on plant growth dynamics, microstructural adaptations, and functional traits. To further investigate the relationship between habitat-specific environmental variables and species responses, heatmap visualizations were generated to illustrate correlations among key ecological parameters. All statistical analyses were performed using R (v 4.0.1) (R Core Team, 2013), ensuring rigorous data interpretation and visualization.

### **Results**

#### **Growth attributes**

##### *Vegetative traits*

Shoot length ( $P < 0.05$ ) was highest in Uch Sharif (agricultural land) from the Cholistan Desert margins (Fig. 2), followed by Bagho Bahar (desert canal) in the Cholistan Desert, while the shortest shoot length was observed in Khan Pur (wasteland) and Kot Mithan (barren land). Root length was significantly greater in Sardar Garh (saline desert) within the Cholistan Desert, whereas Khanpur (wasteland) from the Cholistan Desert margins showed a reduction in root length. Leaf number was highest in Sardar Garh (saline desert) from the Cholistan Desert, followed by Thull Hamza (roadside) from the Cholistan Desert margins, whereas the lowest leaf number was observed in Fateh Pur Kamal (mud flats) and Bagho Bahar (desert canal). Leaf area was largest in Uch Sharif (agricultural land) from the Cholistan Desert margins, followed by Fateh Pur Kamal (mud flats) in the Cholistan Desert, while the smallest leaf area was recorded in Khan Pur (wasteland) and Thull Hamza (roadside). The number of thorns per leaf was highest in Fateh Pur Kamal (mud flats) within the Cholistan Desert, while it was lowest in Khan Pur (wasteland) from the Cholistan Desert margins.

##### *Reproductive traits*

The number of flowers per plant was greatest in Uch Sharif (agricultural land) from the Cholistan Desert margins, whereas it was lowest in Rahim Yar Khan (sand dunes) from the Cholistan Desert. Inflorescence length was longest in Bagho Bahar (desert canal) from the Cholistan Desert and shortest in Khan Pur (wasteland) and Kot Mithan (barren land) from the Cholistan Desert margins. The populations of Thull Hamza (roadside) and Uch Sharif (agricultural land) from the Cholistan Desert margins produced the highest number of fruits, whereas the Rahim Yar Khan (sand dunes) population from the Cholistan Desert exhibited a significantly reduced fruit count.

##### *Biomass production*

Shoot fresh weight was lowest in Bagho Bahar (desert canal) from the Cholistan Desert, whereas Uch Sharif (agricultural land) from the Cholistan Desert margins exhibited the highest shoot fresh weight. Shoot dry weight was highest in Aman Garh (desert flats) from the Cholistan Desert margins and in Bagho Bahar (desert canal) from the Cholistan Desert. The lowest value of this parameter was recorded in Bait Zahir Pir (salt-affected land). Root fresh weight was significantly greater in Uch Sharif (agricultural land) from the Cholistan Desert

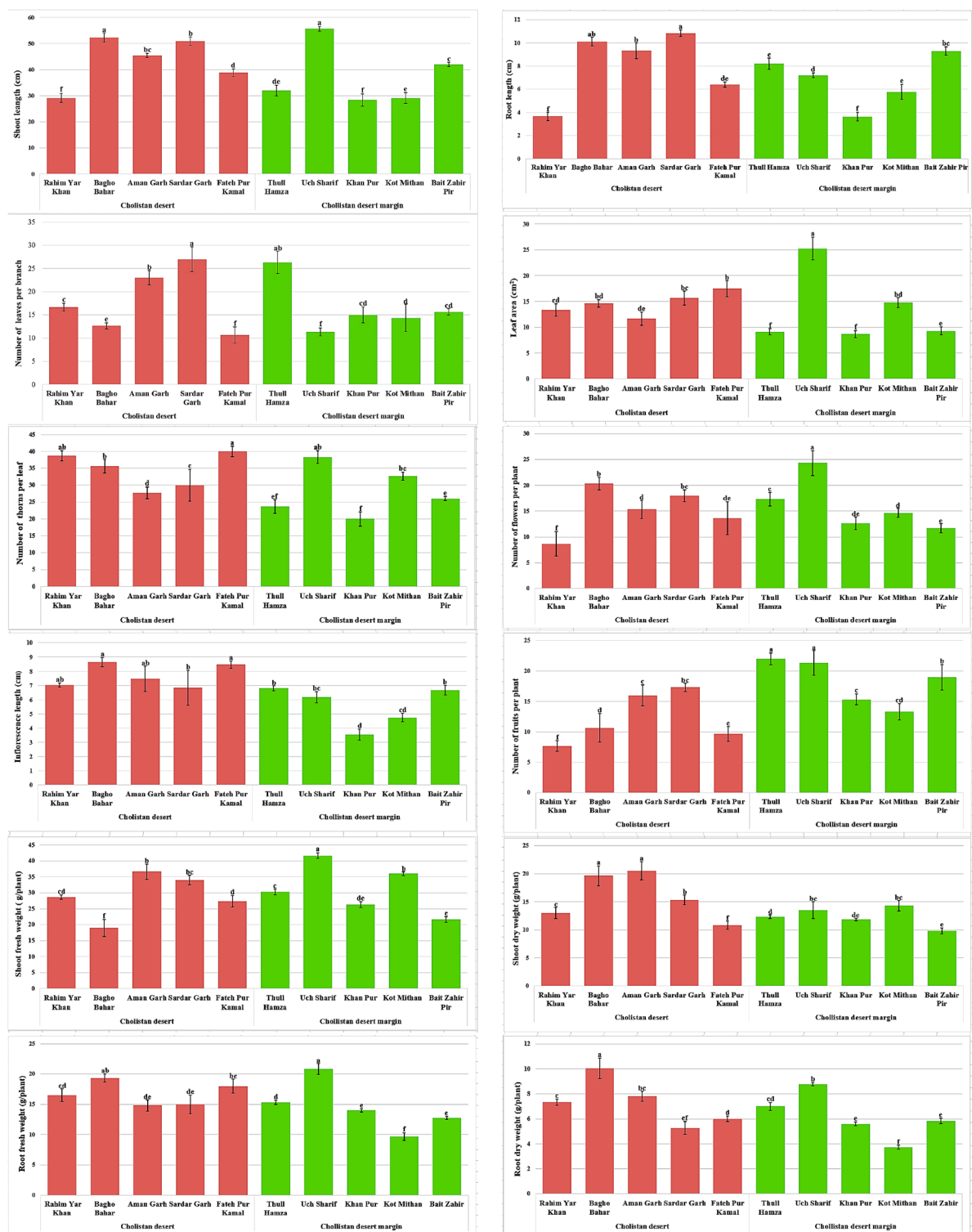


**Fig. 2.** Morphological attributes of *Solanum surattense* sampled from dryland ecosystems. Bars and lines represent mean + SE ( $n = 10$ ). Different letters above bars indicate significant differences ( $P \leq 0.05$ ) across populations in each habitat.



margins, while a decline was noted in Kot Mithan (desert canal) from the Cholistan Desert. Root dry weight was significantly higher in the Bagho Bahar (desert canal) population from the Cholistan Desert, while it was lowest in the Kot Mithan (barren land) population from the Cholistan Desert margins.

Physiological attributes

Osmolyte accumulation

Proline ( $P<0.05$ ) was highest in Aman Garh (desert flats), followed by Bagho Bahar (desert canal), and lowest in Khan Pur (wasteland) and Kot Mithan (barren land) (Table 3). Total soluble sugars were highest in Aman Garh (desert flats), followed by Bagho Bahar (desert canal), and lowest in Khan Pur (wasteland) and Kot Mithan (barren land). Total free amino acids were highest in Aman Garh (desert flats), followed by Bagho Bahar (desert canal), and lowest in Khan Pur (wasteland) and Kot Mithan (barren land).

Photosynthetic pigment traits

Chlorophyll a was highest in Thull Hamza (roadside) and Uch Sharif (agriculture land) in the Cholistan Desert margins, while it was lowest in Khan Pur (wasteland) and Kot Mithan (barren land). Chlorophyll b was highest in Uch Sharif (agriculture land) and Thull Hamza (roadside) and lowest in Kot Mithan (barren land) and Khan Pur (wasteland). Chlorophyll a/b ratio was highest in Kot Mithan (barren land) and Bait Zahir Pir (salt-affected land) and lowest in Sardar Garh (saline desert). Carotenoids were highest in Thull Hamza (roadside) and Kot Mithan (barren land) and lowest in Khan Pur (wasteland) and Rahim Yar Khan (sand dunes). Total chlorophyll was highest in Kot Mithan (barren land) and Uch Sharif (agriculture land) and lowest in Khan Pur (wasteland) and Sardar Garh (saline desert). Carotenoids/chlorophyll ratio was highest in Sardar Garh (saline desert) and lowest in Khan Pur (wasteland) and Rahim Yar Khan (sand dunes).

Anatomical attributes

Root anatomy of plants

**Dermal tissues** Root area ( $P<0.05$ ) exhibited maximum expansion in Thull Hamza (roadside), followed by Khan Pur (wasteland), whereas minimal development was observed in Bait Zahir Pir (salt-affected land) and Sardar Garh (saline desert) (Figs. 3 and 4). Epidermal thickness peaked in Aman Garh (desert flats), with Bagho Bahar (desert canal) showing a slightly lower value, while Rahim Yar Khan (sand dunes) and Sardar Garh (saline desert) exhibited the least epidermal reinforcement.

**Storage tissues** Cortical thickness reached its highest levels in Thull Hamza (roadside) and Uch Sharif (agriculture land), whereas Bagho Bahar (desert canal) and Bait Zahir Pir (salt-affected land) displayed the most reduced cortical layers. Cortical cell area was most extensive in Bagho Bahar (desert canal) and Bait Zahir Pir (salt-affected land), while the smallest dimensions were recorded in Uch Sharif (agriculture land) and Sardar Garh (saline desert).

**Vascular tissues** Vascular bundle area was most pronounced in Bait Zahir Pir (salt-affected land), Khan Pur (wasteland), and Kot Mithan (barren land), whereas it remained at minimal levels in Fateh Pur Kamal (mud flats) and Rahim Yar Khan (sand dunes). Metaxylem area displayed the greatest expansion in Bagho Bahar (desert canal) and Aman Garh (desert flats), whereas Sardar Garh (saline desert) exhibited the most restricted metaxylem development. Phloem area was most pronounced in Bait Zahir Pir (salt-affected land), whereas Uch Sharif (agriculture land) exhibited the lowest phloem structural investment.

Ecological regions	Cholistan desert					Cholistan desert margins				
Collection sites	Rahim Yar Khan	Bagho Bahar	Aman Garh	Sardar Garh	Fateh Pur Kamal	Thull Hamza	Uch Sharif	Khan Pur	Kot Mithan	Bait Zahir Pir
Proline ( $\mu\text{mol g}^{-1}\text{ fw.}$ )	30.93 $\pm$ 1.2c	39.00 $\pm$ 1.5b	39.65 $\pm$ 1.6a	23.26 $\pm$ 1.1de	23.89 $\pm$ 1.0de	29.37 $\pm$ 1.3c	24.98 $\pm$ 1.2d	22.17 $\pm$ 0.9e	22.77 $\pm$ 1.0e	25.66 $\pm$ 1.1d
Total soluble sugar ( $\mu\text{mol g}^{-1}\text{ fw.}$ )	10.45 $\pm$ 0.6c	12.61 $\pm$ 0.7b	13.39 $\pm$ 0.8a	8.98 $\pm$ 0.5f	9.54 $\pm$ 0.6e	11.02 $\pm$ 0.7d	11.28 $\pm$ 0.7d	7.00 $\pm$ 0.4 g	7.44 $\pm$ 0.5 g	8.59 $\pm$ 0.5 h
Total free amino acid ( $\mu\text{mol g}^{-1}\text{ fw.}$ )	17.43 $\pm$ 0.8d	21.96 $\pm$ 1.0b	22.35 $\pm$ 1.1a	17.86 $\pm$ 0.9d	19.06 $\pm$ 0.9c	19.62 $\pm$ 0.9c	17.76 $\pm$ 0.8d	13.93 $\pm$ 0.6e	14.87 $\pm$ 0.7f	15.30 $\pm$ 0.7f
Chlorophyll a ( $\text{mg g}^{-1}\text{ fw.}$ )	1.44 $\pm$ 0.09c	1.40 $\pm$ 0.08d	0.98 $\pm$ 0.06e	0.87 $\pm$ 0.05f	0.80 $\pm$ 0.04 g	1.49 $\pm$ 0.10b	1.62 $\pm$ 0.11a	0.70 $\pm$ 0.03 h	0.69 $\pm$ 0.03i	0.54 $\pm$ 0.02j
Chlorophyll b ( $\text{mg g}^{-1}\text{ fw.}$ )	1.17 $\pm$ 0.07b	1.15 $\pm$ 0.06c	0.64 $\pm$ 0.04f	0.62 $\pm$ 0.04 g	0.49 $\pm$ 0.03 h	1.18 $\pm$ 0.08a	1.24 $\pm$ 0.09a	0.42 $\pm$ 0.02j	0.26 $\pm$ 0.01i	0.27 $\pm$ 0.01i
Chlorophyll a/b ( $\text{mg g}^{-1}\text{ fw.}$ )	1.23 $\pm$ 0.05 h	1.21 $\pm$ 0.04 g	1.53 $\pm$ 0.07e	1.41 $\pm$ 0.06f	1.63 $\pm$ 0.08d	1.26 $\pm$ 0.05f	1.30 $\pm$ 0.06f	1.68 $\pm$ 0.09c	2.68 $\pm$ 0.12a	1.98 $\pm$ 0.10b
Carotenoid ( $\text{mg g}^{-1}\text{ fw.}$ )	0.23 $\pm$ 0.01d	0.23 $\pm$ 0.01d	0.23 $\pm$ 0.01d	0.29 $\pm$ 0.02c	0.29 $\pm$ 0.02c	0.40 $\pm$ 0.02a	0.29 $\pm$ 0.02c	0.20 $\pm$ 0.01e	0.30 $\pm$ 0.02b	0.26 $\pm$ 0.01d
Total chlorophyll ( $\text{mg g}^{-1}\text{ fw.}$ )	2.40 $\pm$ 0.10d	2.36 $\pm$ 0.09d	2.17 $\pm$ 0.08f	2.02 $\pm$ 0.07 g	2.12 $\pm$ 0.08f	2.44 $\pm$ 0.11c	2.54 $\pm$ 0.12b	2.10 $\pm$ 0.08f	2.94 $\pm$ 0.14a	2.25 $\pm$ 0.09e
Carotenoid/chlorophyll ( $\text{mg g}^{-1}\text{ fw.}$ )	0.10 $\pm$ 0.01e	0.10 $\pm$ 0.01e	0.11 $\pm$ 0.01d	0.15 $\pm$ 0.02a	0.14 $\pm$ 0.02b	0.12 $\pm$ 0.01c	0.11 $\pm$ 0.01d	0.10 $\pm$ 0.01e	0.10 $\pm$ 0.01e	0.12 $\pm$ 0.01c

**Table 3.** Physiological parameters of *Solanum surattense* sampled from dryland ecosystems. Values are mean  $\pm$  se ( $n = 10$ ). Mean values in a row with different superscript letters are significantly different ( $p < 0.05$  of the analysis of variance –ANOVA-across sites and post-hoc least significant difference –LSD-test of multiple comparisons among sites).

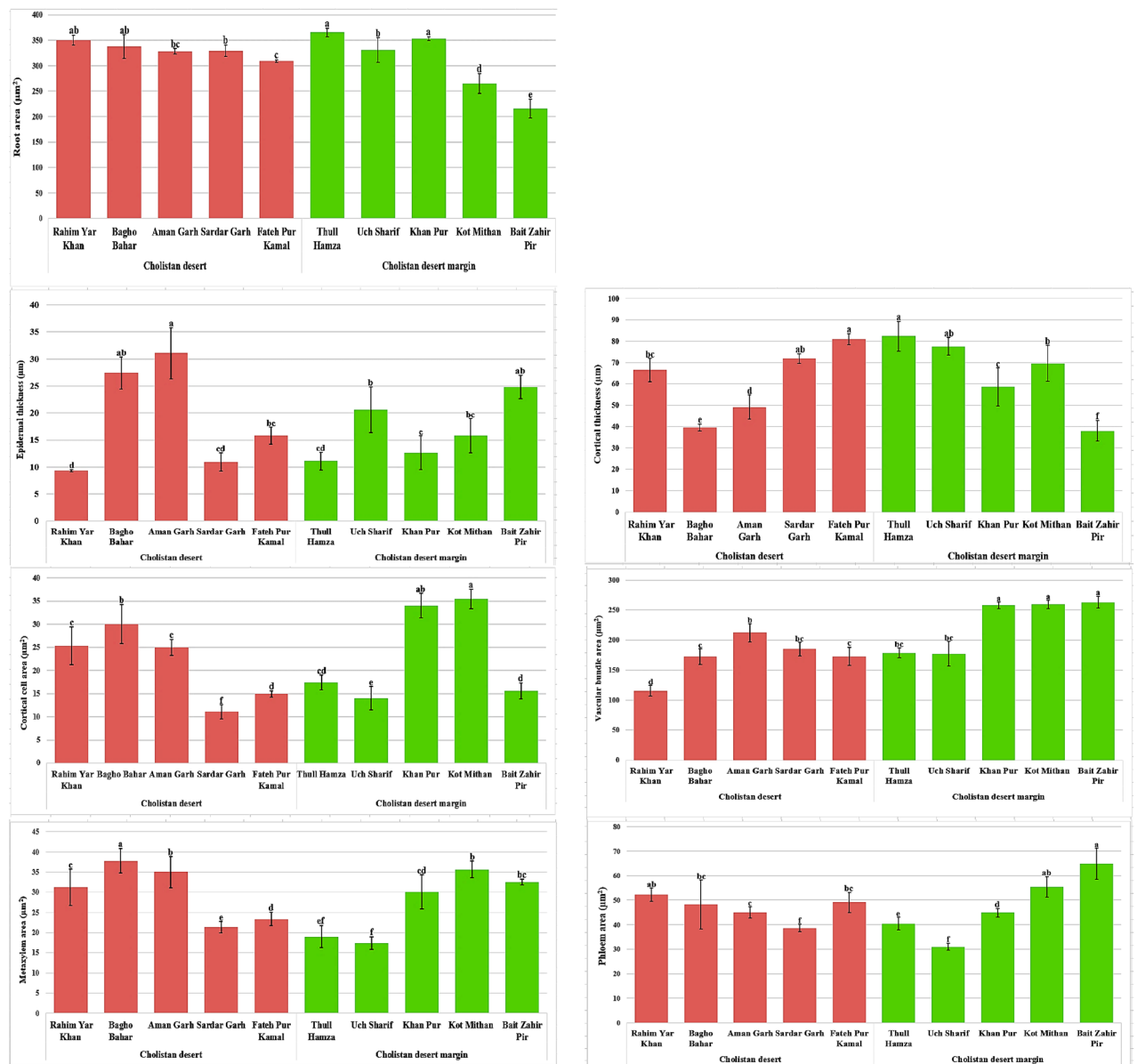


**Fig. 3.** Root anatomical attributes of *Solanum surattense* sampled from dryland ecosystems. Bars and lines represent mean + SE ( $n = 10$ ). Different letters above bars indicate significant differences ( $P \leq 0.05$ ) across populations in each habitat.

#### Stem anatomy of plants

**Dermal tissues** Stem area ( $P < 0.05$ ) was greatest in Bagho Bahar (desert canal), followed by Kot Mithan (barren land), whereas it was lowest in Rahim Yar Khan (sand dunes) and Aman Garh (desert flats) (Figs. 5 and 6). Epidermal thickness was highest in Bagho Bahar (desert canal) and Kot Mithan (barren land) and lowest in Sardar Garh (saline desert) and Khan Pur (wasteland).

**Storage tissues** Cortical thickness reached maximum values in Bagho Bahar (desert canal) and Kot Mithan (barren land) but was reduced in Fateh Pur Kamal (mud flats) and Rahim Yar Khan (sand dunes). Cortical cell area was greatest in Bagho Bahar (desert canal), whereas it was least in Thull Hamza (roadside) and Uch Sharif (agriculture land). Collenchyma thickness was highest in Kot Mithan (barren land) but lowest in Bagho Bahar (desert canal). Pith thickness was greatest in Bagho Bahar (desert canal) but smallest in Khan Pur (wasteland). Pith cell area reached its highest levels in Bagho Bahar (desert canal) and Rahim Yar Khan (sand dunes) and was lowest in Khan Pur (wasteland).

**Vascular tissues** Vascular bundle area was largest in Bagho Bahar (desert canal) but lowest in Rahim Yar Khan (sand dunes) and Sardar Garh (saline desert). Metaxylem area was most extensive in Khan Pur (wasteland),

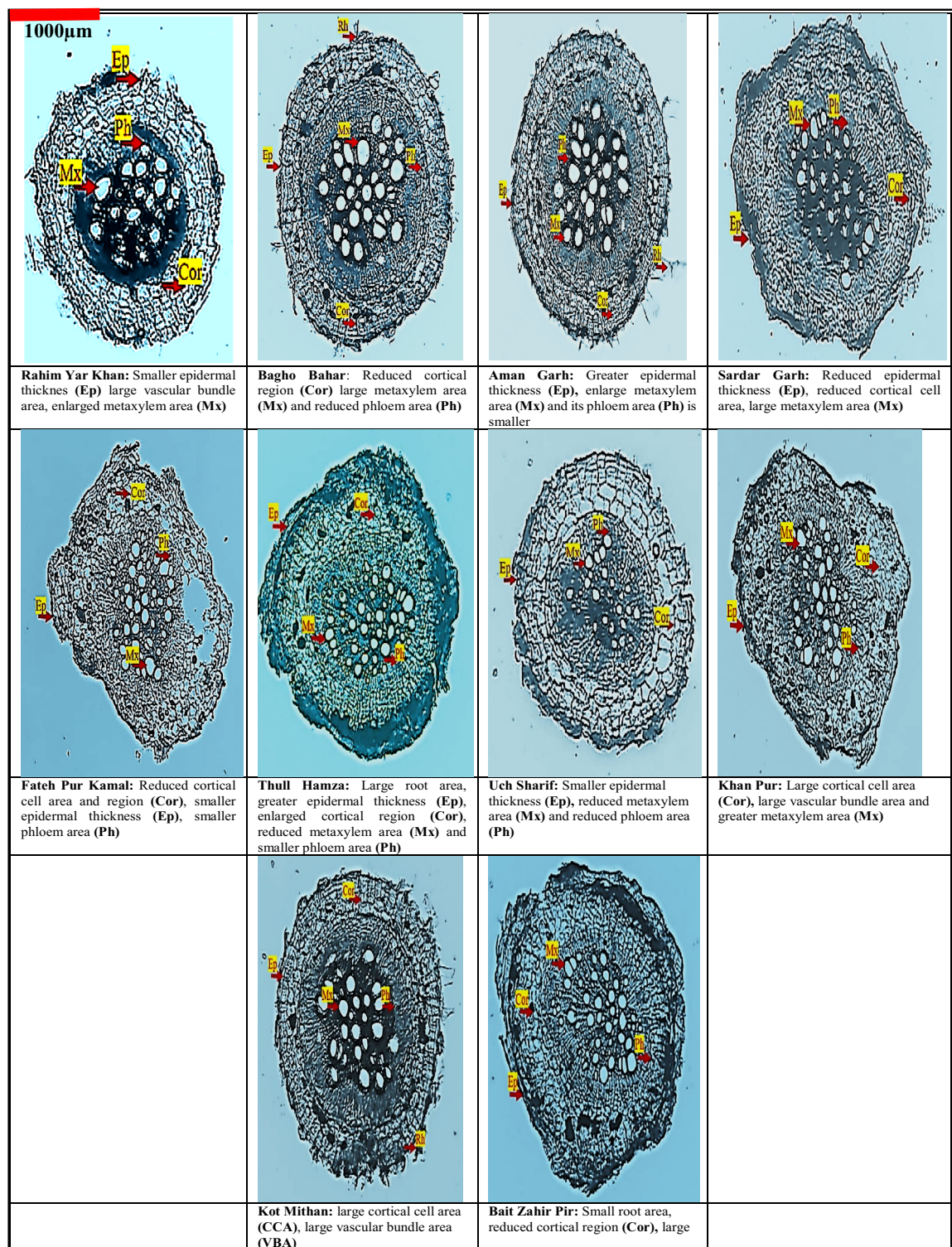


**Fig. 4.** Root transverse sections of *Solanum surattense* sampled from dryland ecosystems. The arrowheads in each panel indicate the specific adaptation of species to their environment ( $n = 10$ ,  $M = 40\times$ ).

while the smallest dimensions were recorded in Thull Hamza (roadside). Phloem area was highest in Uch Sharif (agriculture land) but was reduced in Thull Hamza (roadside).

#### Leaf anatomy of plants

**Dermal tissues** Midrib thickness ( $P < 0.05$ ) was greatest in Rahim Yar Khan (sand dunes), whereas it was lowest in Thull Hamza (roadside) (Figs. 7, 8 and 9). Lamina thickness was highest in Bagho Bahar (desert canal) but lowest in Thull Hamza (roadside). Epidermal thickness was greatest in Aman Garh (desert flats) and smallest in



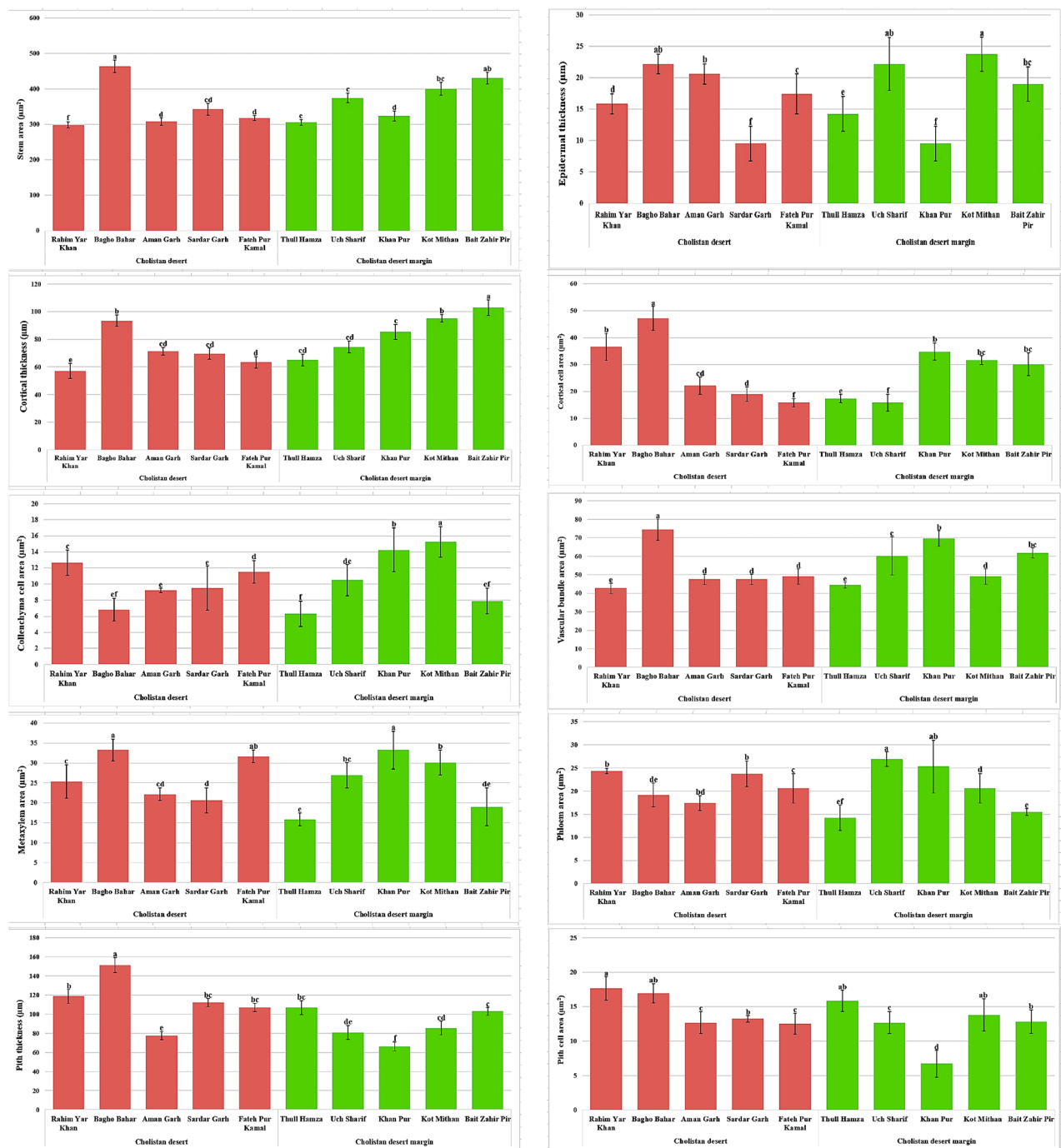


**Fig. 5.** Stem anatomical attributes of *Solanum surattense* sampled from dryland ecosystems. Bars and lines represent mean + SE ( $n = 10$ ). Different letters above bars indicate significant differences ( $P \leq 0.05$ ) across populations in each habitat.

Bagho Bahar (desert canal). Stomatal number was greatest in Aman Garh (desert flats) but lowest in Rahim Yar Khan (sand dunes) Stomatal area was highest in Thull Hamza (roadside) but smallest in Khan Pur (wasteland) and Aman Garh (desert flats).

**Storage tissues** Cortical thickness was most pronounced in Rahim Yar Khan (sand dunes) and Aman Garh (desert flats) but reduced in Fateh Pur Kamal (mud flats). Cortical cell area was highest in Sardar Garh (saline desert) and Rahim Yar Khan (sand dunes) but lowest in Bait Zahir Pir (salt-affected land).

**Vascular tissues** Vascular bundle area was greatest in Khan Pur (wasteland), whereas it was smallest in Thull Hamza (roadside). Metaxylem area was highest in Kot Mithan (barren land) but lowest in Bagho Bahar (desert

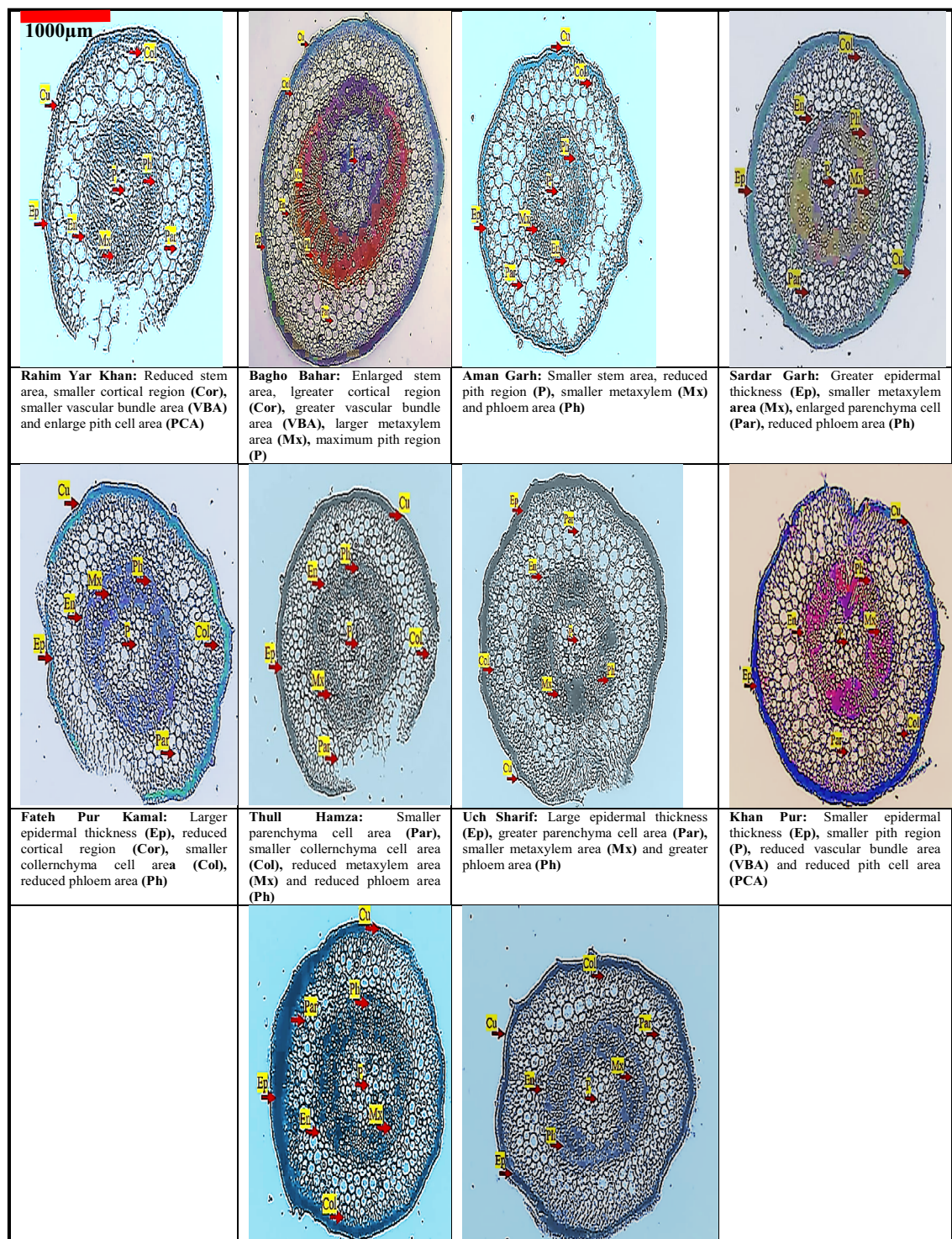


**Fig. 6.** Stem transverse sections of *Solanum surattense* sampled from dryland ecosystems. The arrowheads in each panel indicate the specific adaptation of species to their environment ( $n = 10$ ,  $M = 40\times$ ).

canal). Phloem area was most extensive in Aman Garh (desert flats) and Sardar Garh (saline desert), whereas it was least in Thull Hamza (roadside).

### Results for multivariate analysis

#### Principal component analysis (PCAs)

Principal component analyses (PCA-biplot) of growth and physiological attributes and anatomical traits of *S. surattense* were conducted in relation to edaphic and climatic factors across different habitats (Fig. 10a,b). Root

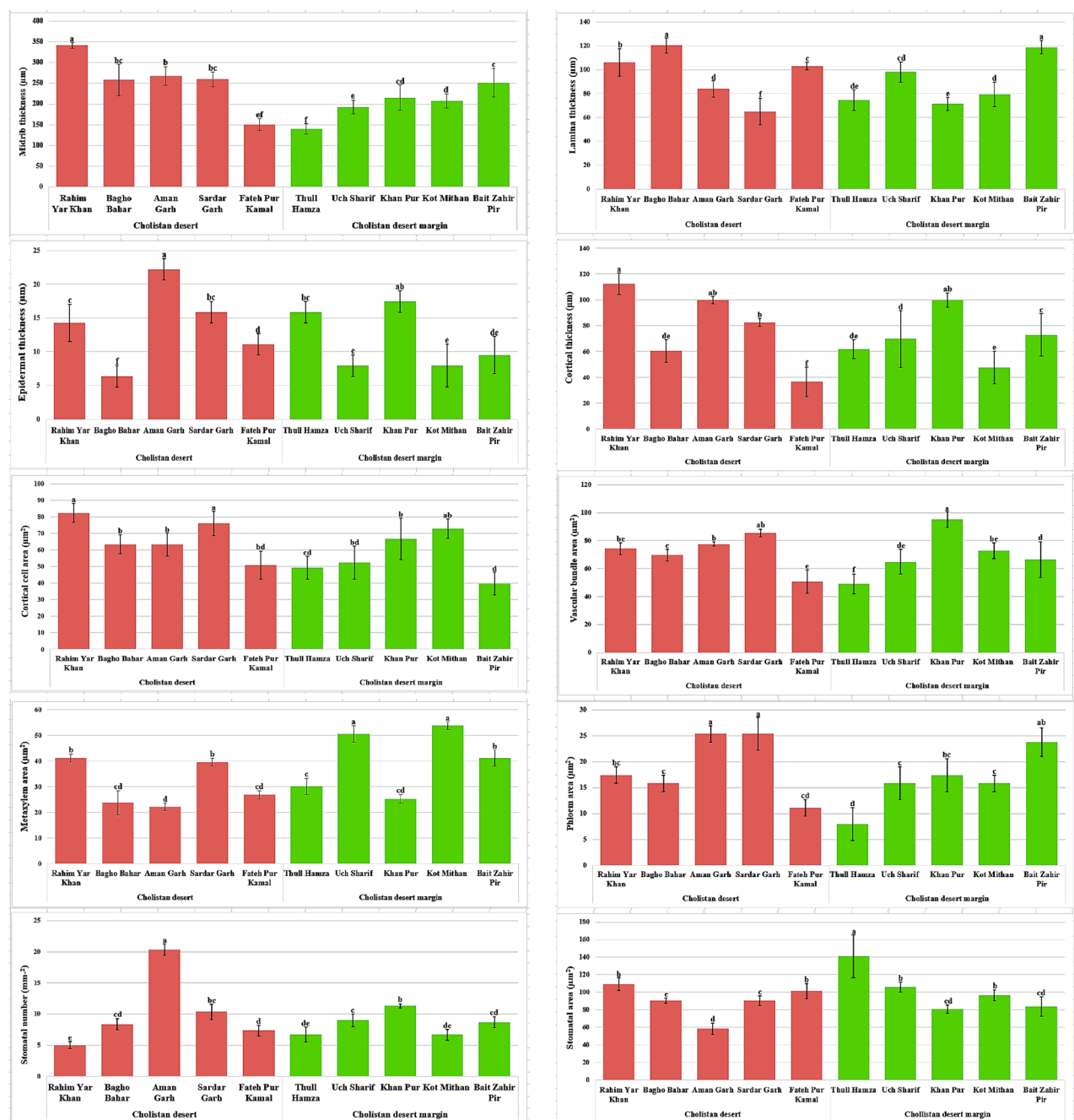


**Fig. 7.** Leaf anatomical attributes of *Solanum surattense* sampled from dryland ecosystems. Bars and lines represent mean + SE ( $n = 10$ ). Different letters above bars indicate significant differences ( $P \leq 0.05$ ) across populations in each habitat.

fresh weight, root dry weight, shoot fresh weight, shoot dry weight, total free amino acids, and shoot length were significantly associated with soil factors, including nitrate, sodium, calcium, and pH. Electrical conductivity and organic matter correlated with Sardar Garh, Bagho Bahar, and Aman Garh. Chlorophyll a, chlorophyll b, total chlorophyll, total soluble sugars, and the carotenoid-to-chlorophyll ratio were significantly linked to Kot Mithan, Rahim Yar Khan, and Uch Sharif. Total soluble sugars and proline content exhibited strong associations with Kot Mithan and Rahim Yar Khan. Leaf epidermal thickness, root cortical cell area, and stem vascular bundle area clustered under the Aman Garh and Bagho Bahar habitats. Soil phosphate and potassium were strongly associated with leaf phloem area and root cortical cell area in the Khan Pur and Uch Sharif habitats. Soil electrical conductivity, sodium, and calcium formed a distinct cluster with stem metaxylem area and leaf metaxylem area under the Kot Mithan and Rahim Yar Khan habitats. Additionally, soil organic matter, nitrate, and saturation percentage are clustered with root metaxylem area and leaf cortical thickness under the Bait Zahir Pir and Fateh Pur Kamal habitats.



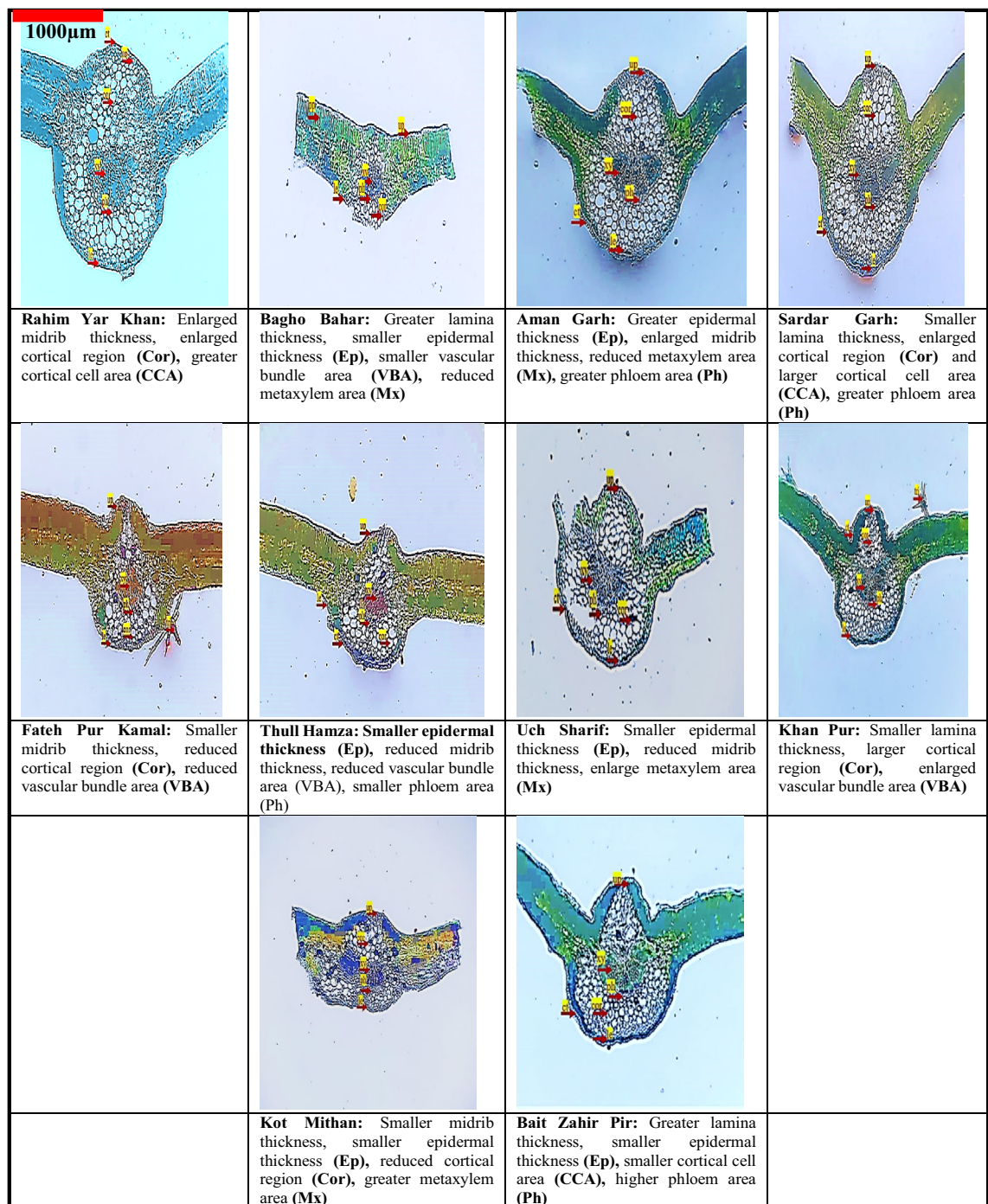


**Fig. 8.** Leaf transverse sections of *Solanum surattense* sampled from dryland ecosystems. The arrowheads in each panel indicate the specific adaptation of species to their environment ( $n = 10$ ,  $M = 40\times$ ).

#### Two-way clustered heatmaps

The clustered heatmap on soil and morpho-physiological traits revealed a strong association and grouping of TChl, Chl a/b, and  $\text{Ca}^{2+}$  in Kot Mithan habitat (Fig. 11a). Soil ECe, OM,  $\text{Na}^+$ , and pH showed clustering in Bait Zahir Pir and Thull Hamza habitats. A weak association was observed among traits such as IDM, Rf, RH,  $\text{NO}_3^-$ ,  $\text{PO}_4^{3-}$ , SP, and ECe in Fateh Pur Kamal and Sardar Garh habitats. The traits TFA, TSS, Pro, and SDW showed a positive relationship with Bagho Bahar and Aman Garh, while traits such as  $\text{Na}^+$ , ECe, OM, and pH exhibited a negative association in Thull Hamza and Bait Zahir Pir habitats. Moreover, traits such as Chl a, Chl b, and RFW showed positive association with Uch Sharif habitat, whereas LN, RL, and SL demonstrated close association with Sardar Garh habitat. In addition, traits LA and SFW showed positive association with Uch Sharif and a negative association with Bait Zahir Pir habitats.

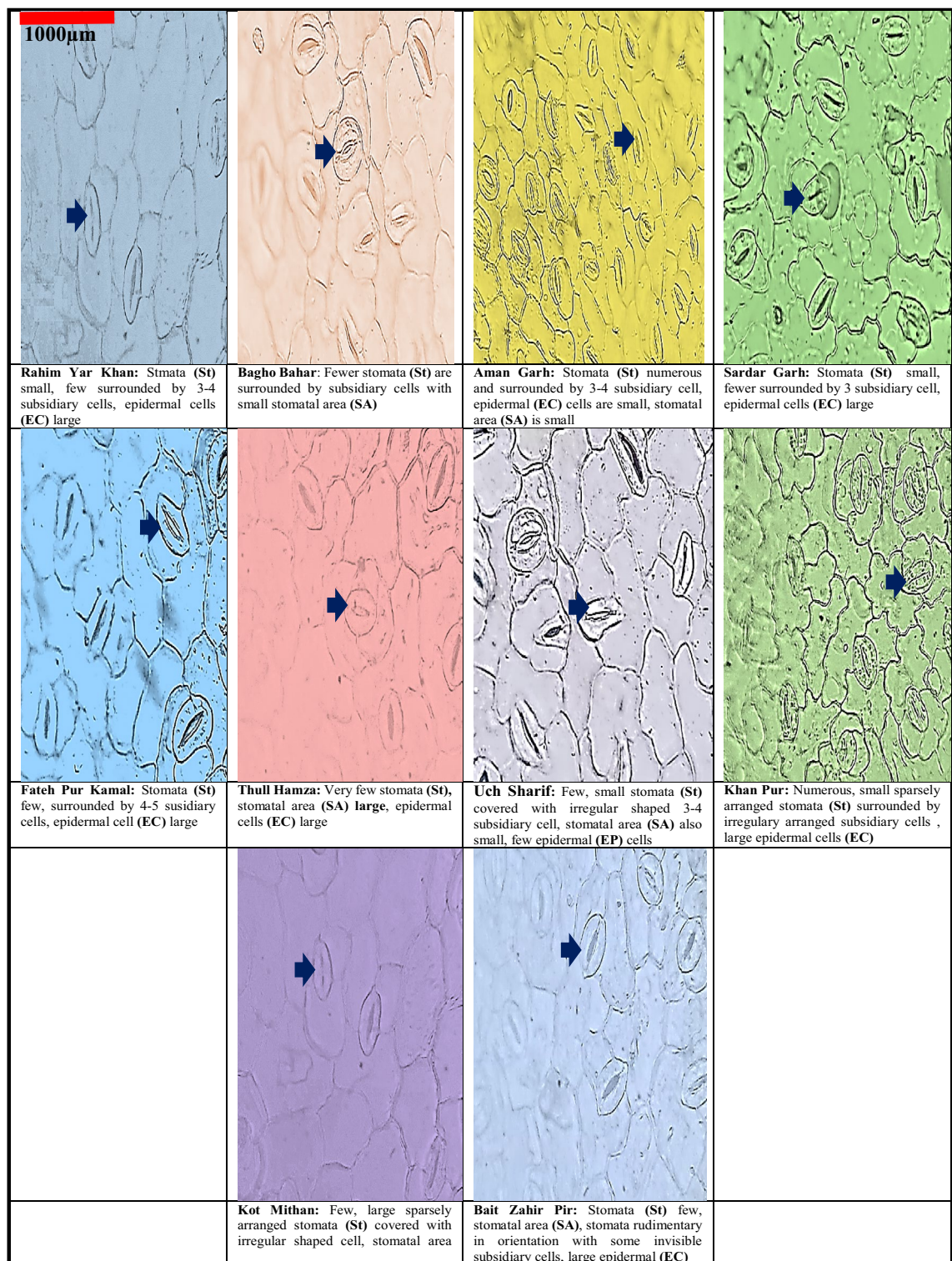
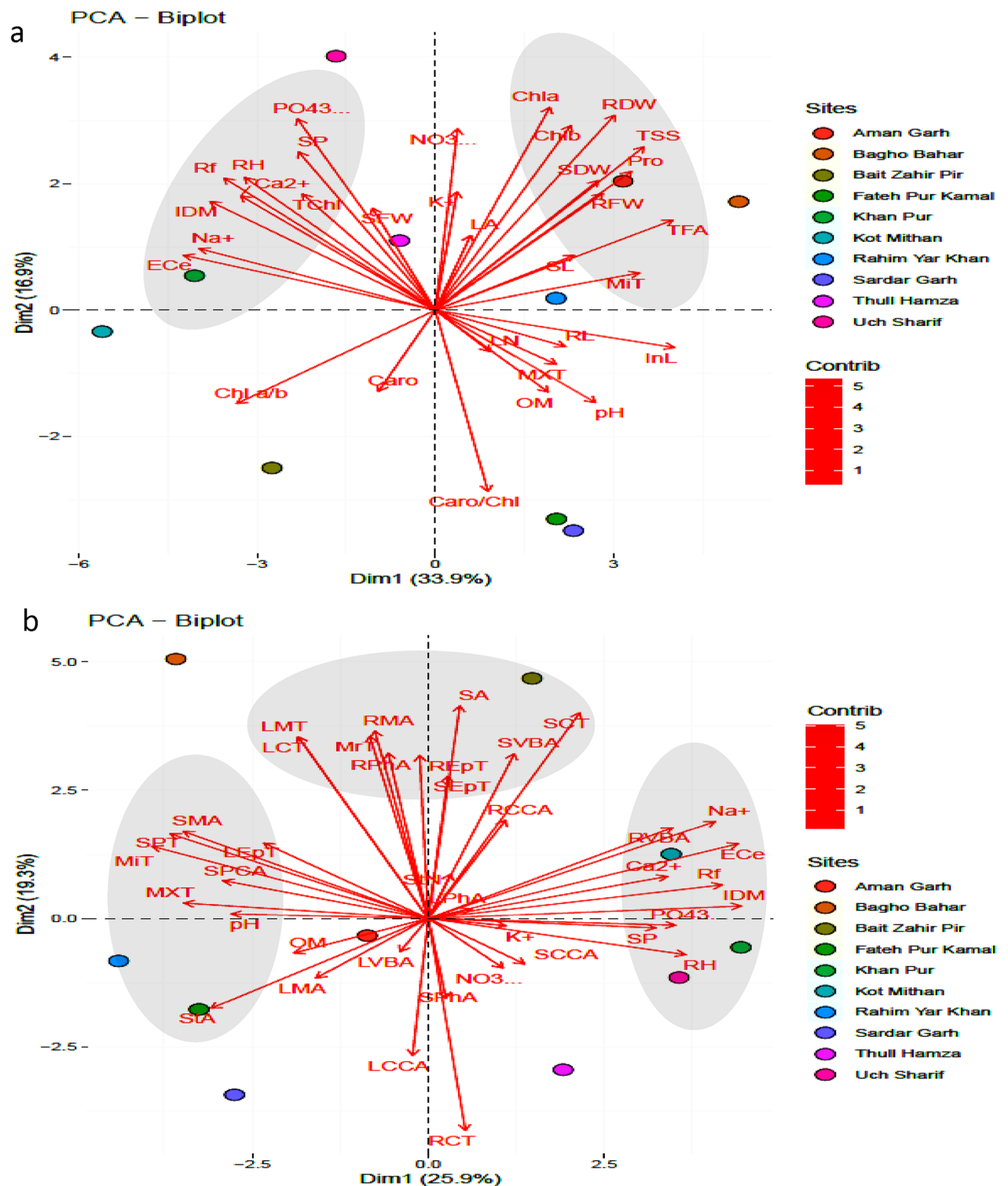


**Fig. 9.** Leaf dermal surface transverse sections of *Solanum surattense* sampled from dryland ecosystems. The arrowheads in each panel indicate the specific adaptation of species to their environment ( $n = 10$ ,  $M = 40\times$ ).

The clustered heatmap on soil and anatomical traits revealed a strong association and grouping of  $\text{PO}_4$ ,  $\text{Ca}^{2+}$ , SP, Rf, RH, and IDM in the Kot Mithan and Uch Sharif habitats (Fig. 11b). A positive association was observed among  $\text{NO}_3$ , K, LCCA, LVBA, LPhA, and SCCA in the Khan Pur habitat, while MXT, LEpT, and MiT were closely associated with the Rahim Yar Khan habitat. Traits such as SA, SCT, EpT, SPT, SPCA, SMA, RepT, LCT, and LMT showed strong association with the Bagho Bahar habitat, whereas StA, RCT, and OM were strongly associated with the Fateh Pur Kamal habitat. Additionally, SVBA,  $\text{NO}_3$ , and K showed a positive association with





both Aman Garh and Khan Pur habitats. In contrast, a negative association of multiple variables—including ECe,  $\text{Na}^+$ , IDM,  $\text{Ca}^{2+}$ , Rf, RH, and RVBA—was observed with the Fateh Pur Kamal and Bagho Bahar habitats.

## Discussion

Ecological indicators derived from plant functional traits are increasingly recognized as robust tools for assessing the impacts of increasing aridity on dryland ecosystems<sup>35</sup>. The ability of plant species to persist under shifting climatic regimes is fundamentally linked to their adaptive strategies for maintaining growth, reproduction, and survival<sup>36</sup>. Among these, functional trait metrics have gained prominence for their strong predictive power in relation to plant responses to environmental stressors<sup>37–39</sup>. The environmental/climatic factors are strongly related to plant functional traits<sup>40–42</sup>. Evolutionary processes have driven the emergence of resilient plant ecotypes, equipping them with specialized structural and physiological adaptations that enhance survival under



◀ **Fig. 10.** Principal component analysis (PCAs) of growth and physiology (a), and anatomical (b) attributes of *Solanum surratense* sampled from dryland ecosystems. The x-axis (Dim1) explains 25.9% of the variance, while the y-axis (Dim2) explains 19.3% of the variance. Red arrows represent environmental variables, where the length and direction indicate their contribution to the principal components. The color intensity of arrows corresponds to the contribution level (Contrib), with darker red indicating higher influence. Different colored circles represent sampling sites. *Soil:* pH Soil pH, SP Saturation percentage, OM Organic matter percentage, *Ece* Electrical conductivity,  $K^+$  Potassium ions,  $Na^+$  Sodium ions,  $Ca^{2+}$  Calcium ions,  $NO_3^-$  Nitrate ions,  $PO_4^{3-}$  Phosphate ions, *Growth:* SL Shoot length, RT Root length, LN Leaf numbers, LA Leaf area, InL Inflorescence length, SFW Shoot fresh weight, RFW Root fresh weight, SDW Shoot dry weight, RDW Root dry weight, RA Root area, *Root:* REpT Epidermal thickness, RCT Cortical thickness, RCCA Cortical cell area, RVBA Vascular bundle area, RMA Metaxylem area, RPhA Phloem area, *Stem:* SA Stem area, SEpT Epidermal thickness, SCT Cortical thickness, SCCA Cortical cell area, SVBA Vascular bundle area, SMA Metaxylem area, SPhA Phloem area, SPT Pith thickness, SPCA Pith cell area, *Leaf:* Mrt Midrib thickness, LMT Lamina thickness, LET Leaf epidermal thickness, LCT Leaf cortical thickness, LCCA Leaf cortical cell area, LVBA Leaf vascular bundle area, LMA metaxylem area, LPhA Leaf phloem area, *Pro* proline, TSS total soluble sugars, TFA total free amino acid, *Chla* chlorophyll a, *Chlb* chlorophyll b, *Tchl* total chlorophyll, *Caro* carotenoids, *Chla/b* chlorophyll a/b, *Caro/Chl* carotenoids/chlorophyll.

extreme conditions<sup>43</sup>. The present study explores these adaptive mechanisms in *Solanum surratense*, emphasizing the anatomical and physiological traits that confer resilience in water-limited habitats (Fig. 12). By elucidating these adaptations, our findings contribute to a deeper understanding of plant survival strategies in arid systems and offer a scientific basis for developing targeted conservation and sustainable land management approaches in regions increasingly affected by climate-induced aridity.

### Growth responses of species to aridity

The populations of *S. surratense* exhibited significant variation in morphological traits across different habitats, indicating adaptive differentiation in response to heterogeneous environmental conditions. This phenotypic plasticity reflects the species' capacity to modulate growth and structural traits as a strategy to enhance survival and performance under varying degrees of aridity. The shoot length of *S. surratense* was notably greater in the Cholistan Desert margins, as seen in the Uch Sharif population, whereas it was significantly reduced under the more extreme environmental conditions of the Cholistan Desert, particularly in Khan Pur and Kot Mithan. This variation supports previous research emphasizing that biomass allocation serves as a reliable measure of stress tolerance in *Lasiurus scindicus* and *Cenchrus ciliaris*<sup>43,44</sup>. Root length exhibited habitat-dependent plasticity, with the population from Sardar Garh, located in the Cholistan Desert, showing significantly longer roots. This trend aligns with findings in *Justicia adhatoda*, where increased root length in highly dry environments is recognized as an adaptive strategy to enhance water uptake from deeper soil layers<sup>45</sup>. In contrast, populations in the Cholistan Desert margins, such as Bait Zahir Pir, displayed reduced root length, indicating a lesser reliance on deep rooting compared to those in harsher arid environments. This discrepancy in root development highlights the species' ability to optimize water acquisition strategies based on habitat-specific moisture availability. The root-to-shoot ratio also varied across habitats, with Uch Sharif (Cholistan Desert margins) exhibiting higher root fresh weight than Bagho Bahar (Cholistan Desert). This observation contrasts with the general trend of higher root-to-shoot ratios in extreme arid environments<sup>46,47</sup> suggesting that *S. surratense* modifies biomass allocation to optimize water uptake depending on surface versus deeper water availability. Such plasticity is critical for survival under water-limited conditions, as evidenced by similar strategies in *Cenchrus setigerus*<sup>48</sup>.

Biomass distribution also varied significantly, with the Aman Garh population from the Cholistan Desert margins displaying the highest shoot dry weight, while populations from Bagho Bahar and Rahim Yar Khan in the Cholistan Desert exhibited the greatest root dry weights. This pattern suggests that biomass production can serve as a key indicator of plant water stress adaptation, where increased root biomass in arid environments facilitates water retention and uptake—an essential survival mechanism in drought-prone ecosystems<sup>43</sup>. Leaf area and leaf number exhibited similar adaptive trends, with the largest leaf area recorded in populations from the Cholistan Desert margins, such as Uch Sharif. Conversely, leaf number was highest in the Cholistan Desert, as seen in Sardar Garh. These findings align with broader adaptation patterns observed in stress-tolerant species (*Stipagrostis plumosa*), where plants modulate morphological traits to optimize photosynthetic efficiency and water conservation under arid conditions<sup>44</sup>. The increased leaf number in arid populations may enhance survival by maximizing photosynthetic potential despite harsh environmental constraints, further reinforcing the adaptive flexibility of *S. surratense* to varying levels of water availability and habitat stress.

### Physiological responses of species to aridity

The physiological responses of *S. surratense* to varying water availability across different habitats highlight its adaptive mechanisms to cope with environmental stress in the Cholistan Desert and its margins. The present study demonstrates a significant increase in proline, total soluble sugars, and total free amino acids in populations from Aman Garh (desert flats) and Bagho Bahar (desert canal) in the Cholistan Desert. These osmolytes play a critical role in osmotic adjustment, allowing plants to maintain cellular turgor and metabolic function under water-deficit conditions<sup>49,50</sup>. This response is consistent with findings that plants in arid environments tend to accumulate higher levels of proline as a protective measure against drought-induced stress<sup>51</sup>. However, populations from Khan Pur (wasteland) and Kot Mithan (barren land), where environmental conditions are more extreme, exhibited lower levels of these osmolytes. This reduction may indicate a physiological threshold

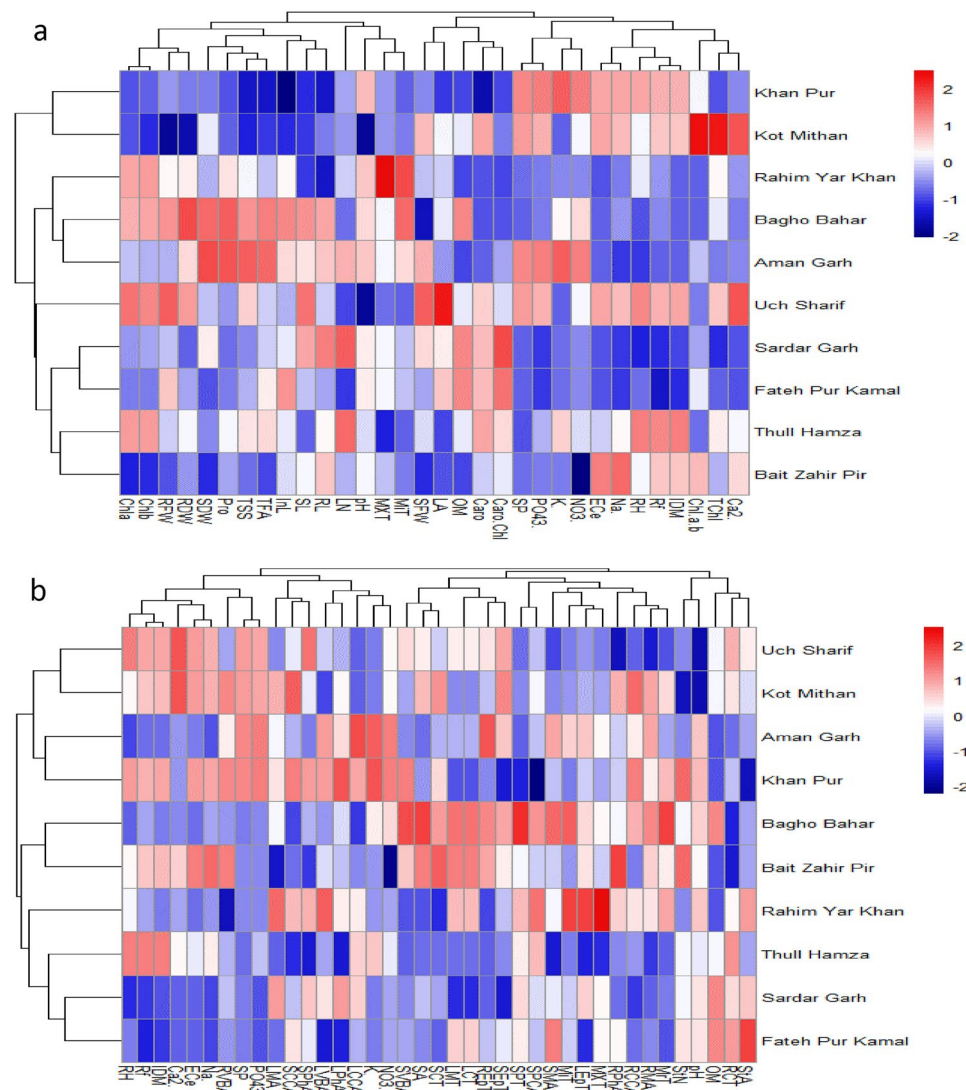


**Fig. 11.** Complex heatmaps showing clustering of growth and physiology (a), and anatomical (b) attributes of *Solanum surratense* sampled from dryland ecosystems. The color scale ranges from -2 (dark blue, indicating low values) to 2 (dark red, indicating high values), with white representing intermediate values. Hierarchical clustering is displayed at the top and left, showing relationships among variables and sites. *Soil:* pH Soil pH, *SP* Saturation percentage, *OM* Organic matter percentage, *Ece* Electrical conductivity, *K<sup>+</sup>* Potassium ions, *Na<sup>+</sup>* Sodium ions, *Ca<sup>2+</sup>* Calcium ions, *NO<sub>3</sub><sup>-</sup>* Nitrate ions, *PO<sub>4</sub><sup>3-</sup>* Phosphate ions, *Growth:* *SL* Shoot length, *RT* Root length, *LN* Leaf numbers, *LA* Leaf area, *InfL* Inflorescence length, *SFW* Shoot fresh weight, *RFW* Root fresh weight, *SDW* Shoot dry weight, *RDW* Root dry weight, *RA* Root area, *Root:* *REpT* Epidermal thickness, *RCT* Cortical thickness, *RCCA* Cortical cell area, *RVBA* Vascular bundle area, *RMA* Metaxylem area, *RPhA* Phloem area, *Stem:* *SA* Stem area, *SEpT* Epidermal thickness, *SCT* Cortical thickness, *SCCA* Cortical cell area, *SVBA* Vascular bundle area, *SMA* Metaxylem area, *SPhA* Phloem area, *SPT* Pith thickness, *SPCA* Pith cell area, *Leaf:* *Mrt* Midrib thickness, *LMT* Lamina thickness, *LET* Leaf epidermal thickness, *LCT* Leaf cortical thickness, *LCCA* Leaf cortical cell area, *LVBA* Leaf vascular bundle area, *LMA* metaxylem area, *LPhA* Leaf phloem area, *Pro* proline, *TSS* total soluble sugars, *TFA* total free amino acid, *Chla* chlorophyll a, *Chlb* chlorophyll b, *Tchl* total chlorophyll, *Caro* carotenoids, *Chla/b* chlorophyll a/b, *Caro/Chl* carotenoids/chlorophyll.

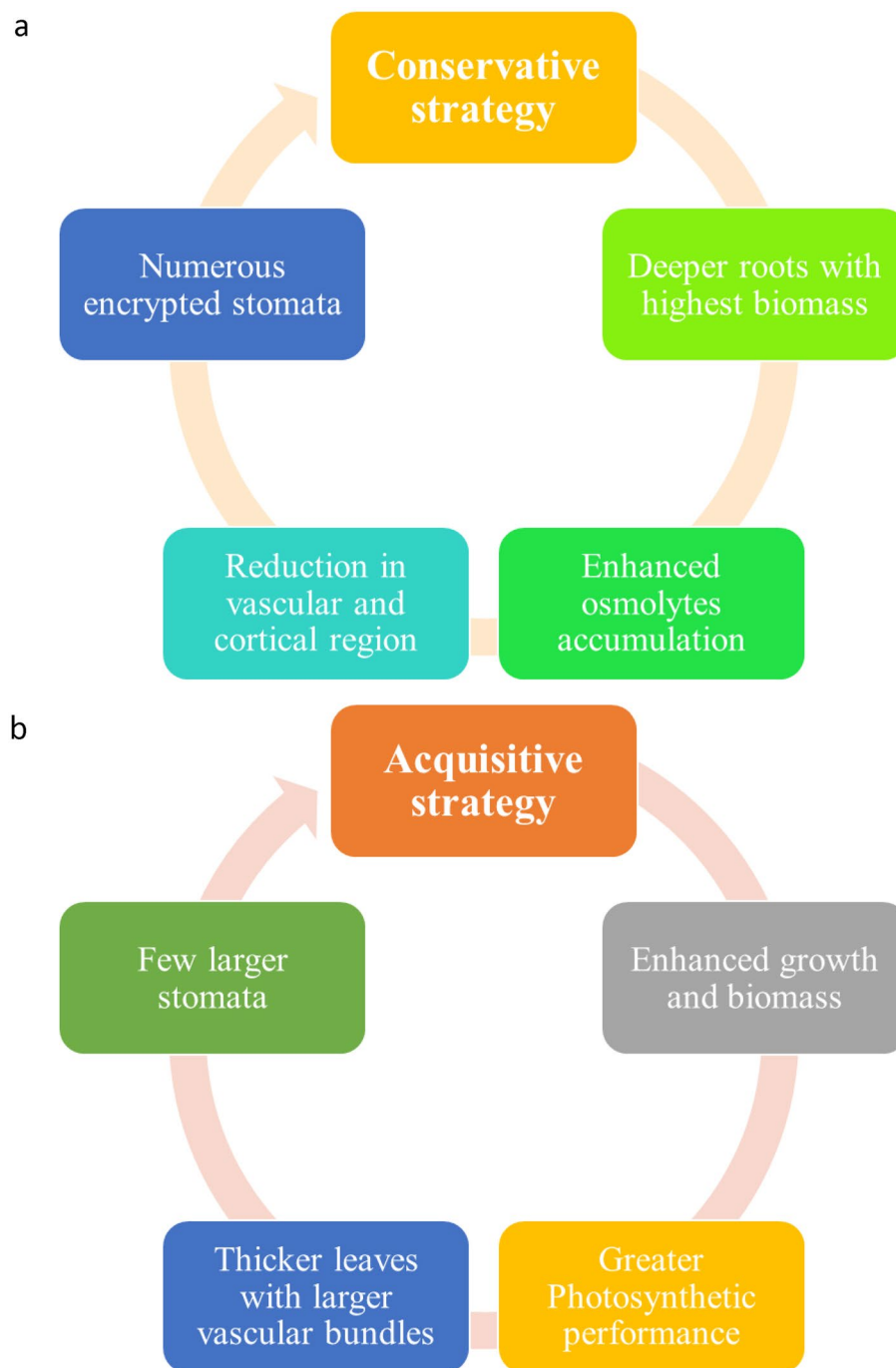


**Fig. 12.** Adaptive strategies of *Solanum surratense* sampled from dryland ecosystems (a-Cholistan Desert, b-Cholistan Desert margins).

The decrease in chlorophyll content in these populations aligns with observations in *Cenchrus ciliaris*, where severe drought conditions led to impaired photosynthesis and pigment breakdown<sup>51</sup>.

Carotenoid levels varied across populations, serving as an important photoprotective mechanism against oxidative damage. Populations from the Cholistan Desert margins, such as Thull Hamza (roadside) and Kot Mithan (barren land), exhibited increased carotenoid concentrations, likely as a defense strategy to counteract oxidative stress. However, in the more extreme conditions of the Cholistan Desert, such as Khan Pur and Rahim Yar Khan, carotenoid levels were lower, suggesting greater susceptibility to photoinhibition. This trend aligns with research indicating that prolonged water stress can impair the biosynthesis of carotenoids, leading to reduced photoprotection and greater vulnerability to oxidative damage in mesophyll and epidermal tissues<sup>54</sup>. The chlorophyll *a/b* ratio showed a significant increase in populations from Kot Mithan and Bait Zahir Pir, indicating a shift in pigment composition in response to water-limited conditions. This ratio is often higher in drought-

stressed plants due to the preferential degradation of chlorophyll *a*, a response that allows plants to optimize light absorption under fluctuating environmental conditions<sup>53</sup>. These findings highlight the physiological plasticity of *S. surratense*, demonstrating its ability to modulate pigment composition and osmolyte accumulation as part of its adaptive strategy to withstand varying degrees of water stress in the Cholistan Desert and its margins.

### Structural responses of species to aridity

The structural adaptations observed in *Solanum surratense* across populations from the Cholistan Desert and its margins exhibit distinct ecophysiological responses to varying aridity levels, particularly in root anatomical traits that parallel those reported in other arid and semi-arid species. Notably, root area was significantly larger in populations from semi-arid margins, such as Thull Hamza (roadside) and Khan Pur (wasteland), suggesting an adaptive strategy to maximize water uptake where water is limited but not absent. In contrast, populations from more extreme arid environments, such as Bait Zahir Pir (salt-affected land) and Sardar Garh (saline desert), exhibited a marked reduction in root area, consistent with growth constraints under severe water stress. This pattern is consistent with adaptive responses reported in other xerophytic species, such as *Withania coagulans*<sup>55</sup> and *Cenchrus ciliaris*<sup>43</sup> which also modulate root morphology to optimize water acquisition under drought-prone conditions.

Further, epidermal and cortical thickness are key indicators of structural resilience to dehydration which were significantly enhanced in populations inhabiting moderately arid zones (e.g., Bagho Bahar and Aman Garh). These features contribute to reduced transpirational loss and improved water retention, aligning with findings in *Justicia adhatoda*, where thickened root epidermis minimized water permeability under stress<sup>45,56</sup>. Similarly, *Calotropis procera* and *Tamarix aphylla* known for their resilience in arid ecosystems, exhibit thickened root and stem tissues to mitigate desiccation risk<sup>57</sup> highlighting a convergent adaptive strategy among drought-tolerant taxa<sup>58,59</sup>.

Cortical cell area, which supports intracellular water storage and reduces tissue metabolic activity, was also greater in populations from moderately arid sites (e.g., Bagho Bahar, Thull Hamza). This trait declined under harsher conditions, such as in Khan Pur and Bait Zahir Pir, mirroring patterns observed in *datura stramonium*<sup>60</sup> and *Panicum antidotale*<sup>61</sup> where reduced cortical development is attributed to resource reallocation under extreme stress<sup>62</sup>.

Furthermore, vascular bundle area, a critical trait for effective water and nutrient transport increased significantly in populations from less arid zones such as Aman Garh (desert flats) and Kot Mithan (barren land). This trend is consistent with findings in *Cenchrus ciliaris*<sup>63</sup> and *Olea europaea*<sup>64</sup> where increased vascular bundle size, particularly metaxylem and phloem, facilitates improved hydraulic conductivity and drought tolerance under similar conditions<sup>65</sup>. Conversely, populations subjected to extreme aridity, such as those from Fateh Pur Kamal and Rahim Yar Khan (sand dunes), exhibited a marked reduction in vascular bundle area, suggesting a resource-conservative strategy under high water stress.

Larger metaxylem vessels in populations from transitional desert margins (e.g., Khan Pur and Bait Zahir Pir) likely represent an adaptive response to moderate aridity, enhancing water transport efficiency through reduced xylem resistance, a feature also documented in xerophytic grasses like *Cenchrus prieurii*, *C. pennisetiformis* and *C. setiger*<sup>66</sup>. Similarly, expansion of the phloem area in populations like Kot Mithan and Uch Sharif support sustained assimilate transport under water-limited conditions, reflecting a strategy observed in drought-adapted halophytes<sup>50,67</sup>. In contrast, reduced phloem areas under harsher environments (e.g., Khan Pur and Rahim Yar Khan) may indicate a trade-off between conductive tissue investment and survival under extreme stress<sup>68</sup>.

Stem anatomical traits further illustrate convergent strategies. Increased stem area, epidermal and cortical thickness, and enhanced pith development in populations from Bagho Bahar (desert canal) and Kot Mithan reflect a typical water storage-enhancing syndrome 62, 63, comparable to that seen in succulent or semi-succulent desert taxa like *Tamarix aphylla* and *Cenchrus ciliaris*<sup>59,69</sup>. These modifications collectively contribute to hydraulic buffering and improved drought resilience<sup>63</sup>. Thus, the anatomical plasticity observed in *S. surratense* aligns with interspecific trends among desert-adapted species, underscoring shared ecological strategies that enhance survival under variable arid conditions.

The significant increase in stem area in the Bagho Bahar population, followed by Kot Mithan, suggests that the expansion of the stem plays a crucial role in water storage and mechanical support in arid regions. However, in extreme aridity, such as in Rahim Yar Khan (dunes) and Aman Garh (desert flats), the stem area decreased, indicating a limitation in water availability, which impacts the plant's ability to maintain larger structural components. Similar responses have been reported in high altitude grasses and desert species where reduced stem area minimizes water loss while maintaining essential metabolic activities<sup>59,70</sup>. Epidermal and cortical thickness were also significantly greater in populations from the Cholistan Desert, particularly in Bagho Bahar and Kot Mithan, suggesting that these populations have developed thicker protective layers to prevent water loss and ensure better survival under dry conditions. The increased cortical thickness in these populations enhances their ability to store water within the stem tissues, a critical adaptation for enduring prolonged periods of drought<sup>55</sup>. In contrast, extreme arid conditions in populations like Sardar Garh and Khan Pur led to a reduction in both epidermal and cortical thickness, indicating that these populations are less equipped to handle severe water stress, much like other species in saline or hyperarid environments where such reductions are vital to minimizing water loss<sup>60</sup>.

The observed leaf anatomical traits in *S. surratense* populations highlight significant adaptive strategies that allow the plant to survive under varying arid conditions. The increased midrib thickness observed in the Rahim Yar Khan (sand dunes) population, followed by Uch Sharif (agriculture land), suggests that these populations have developed thicker midribs to better withstand arid conditions<sup>61</sup>. Thicker midribs, containing more parenchymatous tissue, enhance water retention and mechanical support, which is crucial for survival in extreme environments<sup>60</sup>. However, in extreme arid conditions, such as in Thull Hamza (roadside) and Bait Zahir Pir (salt-



affected land), midrib thickness decreased, possibly reflecting the plant's reduced capacity to retain water under harsher conditions. Lamina thickness was significantly higher in the Bagho Bahar (desert canal) population, followed by Fateh Pur Kamal (mud flats). Thicker lamina is a common adaptation in drought-tolerant plants, as it increases water storage capacity and reduces water loss through transpiration<sup>50</sup>. The reduction in lamina thickness in extreme arid populations like Khan Pur (wasteland) and Thull Hamza indicates the plant's strategy to conserve water by minimizing leaf surface area. This is consistent with previous studies where thinner leaves are associated with reduced transpiration rates in water-limited environments<sup>69</sup>. Stomatal characteristics also play a crucial role in drought tolerance. The increased stomatal number in Rahim Yar Khan and Aman Garh populations suggests that these plants can regulate gas exchange and water loss more effectively under moderate arid conditions. However, in extreme aridity, as seen in Bait Zahir Pir and Kot Mithan, the reduction in stomatal number reflects a strategy to conserve water by minimizing transpiration<sup>59</sup>. Additionally, smaller stomatal size, as observed in populations from extreme arid zones, reduces water requirements for turgor maintenance, further enhancing the plant's ability to withstand water stress<sup>61,71</sup>.

### Implications for conservation and sustainable utilization

The findings of this study have significant implications for the conservation and sustainable use of *S. surratense*, a species with considerable ecological and ethnobotanical value. Its robust drought tolerance mechanisms highlight its potential for use in habitat restoration, soil stabilization, and reforestation programs in arid and semi-arid regions facing desertification. Additionally, given its medicinal properties and traditional use in indigenous medicine, understanding its physiological resilience can inform sustainable harvesting practices to prevent overexploitation. However, anthropogenic pressures, including habitat destruction, overgrazing, and climate change, pose serious threats to wild populations. Conservation strategies must prioritize ex situ and in situ approaches, including seed banking, controlled cultivation, and habitat protection to ensure long-term survival. Further research into genetic diversity and adaptive traits could enhance breeding programs for developing drought-resistant cultivars, contributing to both conservation efforts and agricultural sustainability in water-scarce environments.

### Conclusion

The study of *S. surratense* across the Cholistan Desert and its margins reveals key anatomical and physiological adaptations that confer enhanced drought resilience. Structural modifications, including increased root and vascular bundle areas, contribute to improved water uptake and transport efficiency. The accumulation of osmolytes like proline, glycine betaine, and sugars contribute to cellular protection and osmotic balance under water-deficit conditions. Concurrently, stomatal adjustments optimize the trade-off between carbon assimilation and water conservation. Together, these traits underpin the species' capacity to survive and function in arid environments, offering valuable insights into plant adaptive strategies under escalating drought stress. Future research should explore the genetic and molecular basis of these adaptive traits with the aim of identifying key regulatory pathways involved in drought tolerance. Additionally, integrating these findings into ecosystem restoration and sustainable agricultural practices could support vegetation sustainability in arid landscapes. Predictive modeling *S. surratense* responses under projected climate scenarios may further aid in developing strategies for conserving drought-tolerant species in the face of climate change.

### Data availability

All data supporting the findings of this study are included in the paper.

Received: 2 December 2024; Accepted: 18 June 2025

Published online: 01 July 2025

### References

- Shu, Y., Jiang, L., Liu, F. & Lv, G. Effects of plant diversity and abiotic factors on the multifunctionality of an arid desert ecosystem. *PLoS One*. **17**, e0266320 (2022).
- Zhang, L. et al. Aridity thresholds of microbiome-soil function relationship along a Climatic aridity gradient in alpine ecosystem. *Soil. Biol. Biochem.* **192**, 109388 (2024).
- Delgado-Baquerizo, M. et al. Aridity modulates N availability in arid and semiarid mediterranean grasslands. *PLoS One*. **8**, e59807 (2013).
- Huo, Z., Dai, X., Feng, S., Kang, S. & Huang, G. Effect of climate change on reference evapotranspiration and aridity index in arid region of China. *J. Hydrol.* **492**, 24–34 (2013).
- Gross, N. et al. Uncovering multiscale effects of aridity and biotic interactions on the functional structure of mediterranean shrublands. *J. Ecol.* **101**, 637–649 (2013).
- Voltaire, F., Barkaoui, K. & Norton, M. Designing resilient and sustainable grasslands for a drier future: adaptive strategies, functional traits and biotic interactions. *Europ J. Agron.* **52**, 81–89 (2014).
- Harpole, W. S. & Suding, K. N. A test of the niche dimension hypothesis in an arid annual grassland. *Oecologia* **166**, 197–205 (2011).
- Trenberth, K. E. et al. Global warming and changes in drought. *Nat. Clim. Change*. **4**, 17–22 (2014).
- Berdugo, M. et al. Global ecosystem thresholds driven by aridity. *Science* **367**, 787–790 (2020).
- Maestre, F. T. et al. Plant species richness and ecosystem multifunctionality in global drylands. *Science* **335**, 214–218 (2012).
- Durán, J. et al. Temperature and aridity regulate Spatial variability of soil multifunctionality in drylands across the Globe. *Ecology* **99**, 1184–1193 (2018).
- Stampfli, A., Bloor, J. M., Fischer, M. & Zeiter, M. High land-use intensity exacerbates shifts in grassland vegetation composition after severe experimental drought. *Glob Chang. Biol.* **24**, 2021–2034 (2018).
- Soliveres, S. et al. Plant diversity and ecosystem multifunctionality peak at intermediate levels of Woody cover in global drylands. *Global Ecol. Biogeograp.* **23**, 1408–1416 (2014).

14. Mourya, N., Bargali, K. & Bargali, S. Effect of coriaria Nepalensis wall. Colonization in a mixed conifer forest of Indian central himalaya. *J. Forestry Res.* **30**, 305–317 (2019).
15. Ziffer-Berger, J., Weisberg, P. J., Cablk, M. E. & Osem, Y. Spatial patterns provide support for the stress-gradient hypothesis over a range-wide aridity gradient. *J. Arid Environ.* **102**, 27–33 (2014).
16. Awasthi, P., Bargali, K. & Bargali, S. Relative performance of Woody vegetation in response to facilitation by coriaria Nepalensis in central himalaya, India. *Rus J. Ecol.* **53**, 191–203 (2022).
17. Azam, A. et al. Biomonitoring and phytoremediation potential of *Conocarpus erectus* (Buttonwood) for mitigating air pollution from highway traffic. *Chemosphere* **375**, 144259 (2025).
18. Hammond, W. M. et al. Global field observations of tree die-off reveal hotter-drought fingerprint for earth's forests. *Nat. Commun.* **13**, 1761 (2022).
19. Choat, B. et al. Global convergence in the vulnerability of forests to drought. *Nature* **491**, 752–755 (2012).
20. Bargali, K. & Bargali, S. Germination capacity of seeds of leguminous plants under water deficit conditions: implication for restoration of degraded lands in Kumaun himalaya. *Trop. Ecol.* **57**, 445–453 (2016).
21. Blackman, C. J. et al. Leaf hydraulic vulnerability to drought is linked to site water availability across a broad range of species and climates. *Ann. Bot.* **114**, 435–440 (2014).
22. Tekuri, S. K. et al. Phytochemical and Pharmacological activities of *Solanum surattense* burm. f.—A review. *J. App Pharm. Sci.* **9**, 126–136 (2019).
23. Boomiga, M., Suresh, J., Nalina, L. & Rajamani, K. Taxonomy, crop improvement, chemical composition and in vitro approaches of yellow berried nightshade (*Solanum Surattense* burm. F): A comprehensive review. *Med. Plant. Int. J. Phyto Rel Ind.* **13**, 229–236 (2021).
24. Sahar, A., Aftab, K., Chaudhry, A. H. & Malik, T. A. Phytochemistry and biological importance of *Solanum surattense*. *World Appl. Sci. J.* **36**, 529–536 (2018).
25. Narayanan, M. et al. An in vitro investigation of the antidermatophytic, antioxidant, and nephroprotective activity of *Solanum surattense*. *Process. Biochem.* **109**, 178–185 (2021).
26. Baltas, E. Spatial distribution of Climatic indices in Northern Greece. *Meteorological Applications: J. Pract. App Train. TechniqModel.* **14**, 69–78 (2007).
27. Yoshida, S., Forno, D. A. & Cock, J. H. Laboratory manual for physiological studies of rice. (1971).
28. Kowalenko, C. & Lowe, L. Determination of nitrates in soil extracts. *Soil. Sci. Soc. Amer J.* **37**, 660–660 (1973).
29. Richards, L. A. *Diagnosis and Improvement of Saline and Alkali Soils* (US Government Printing Office, 1954).
30. Sims, J. R. & Haby, V. A. Simplified colorimetric determination of soil organic matter. *Soil. Sci.* **112**, 137–141 (1971).
31. Bates, L. S., Waldren, R. P. & Teare, I. Rapid determination of free proline for water-stress studies. *Plant. Soil.* **39**, 205–207 (1973).
32. Moore, S. & Stein, W. H. Photometric nin-hydrin method for use in the ehromatography of amino acids. *J. Biol. Chem.* **176**, 367–388 (1948).
33. Yemm, E. & Willis, A. The Estimation of carbohydrates in plant extracts by anthrone. *Biochem. J.* **57**, 508 (1954).
34. Arnon, D. I. Copper enzymes in isolated chloroplasts. Polyphenoloxidase in *Beta vulgaris*. *Plant. Physiol.* **24**, 1 (1949).
35. Branquinho, C., Serrano, H. C., Nunes, A., Pinho, P. & Matos, P. Essential biodiversity change indicators for evaluating the effects of anthropocene in ecosystems at a global scale. *Assess. Conserv. Biodiv. Concept. Pract. Challenges* 137–163 (2019).
36. Negi, B., Khatri, K., Bargali, S. S., Bargali, K. & Fartyal, A. Phenological behaviour of *Ageratina adenophora* compared with native herb species across varied habitats in the Kumaun himalaya. *Plant Ecol.* 1–13 (2025).
37. Nunes, A. et al. Which plant traits respond to aridity? A critical step to assess functional diversity in mediterranean drylands. *Agric. For. Meteorol.* **239**, 176–184 (2017).
38. de Oliveira, A. C. P., Nunes, A., Rodrigues, R. G. & Branquinho, C. The response of plant functional traits to aridity in a tropical dry forest. *Sci. Total Environ.* **747**, 141177 (2020).
39. Khatri, K., Negi, B., Bargali, K. & Bargali, S. S. Phenotypic variation in morphology and associated functional traits in *Ageratina adenophora* along an altitudinal gradient in Kumaun himalaya, India. *Biologia* **78**, 1333–1347 (2023).
40. Ergül Bozkurt, A. & Coşkunçelebi, K. Population variability of Scots pine (*Pinus sylvestris* L.) in Turkey according to the needle morphology. *Şumarski List.* **145**, 347–353 (2021).
41. Khatri, K., Negi, B., Bargali, K. & Bargali, S. S. Effects of elevation and habitat on leaf and reproductive traits of *Ageratina adenophora* (Sprengel) King & Robinson. *South. Afric J. Bot.* **147**, 859–870 (2022).
42. Burczyk, W. et al. Does leaf mass per area (LMA) discriminate natural pine populations of different origins? *Eur. J. For. Res.* **141**, 1177–1187 (2022).
43. Ameer, A. et al. Aridity-driven changes in structural and physiological characteristics of Buffel grass (*Cenchrus ciliaris* L.) from different ecozones of Punjab Pakistan. *Physiol. Mol. Biol. Plants.* <https://doi.org/10.1007/s12298-023-01351-3> (2023).
44. Naz, N. et al. Morpho-anatomical and physiological attributes for salt tolerance in Sewan grass (*Lasiurus scindicus* Henr.) from Cholistan desert, Pakistan. *Acta Physiol. Plant.* **36**, 2959–2974 (2014).
45. Matloob, H. & Hameed, M. Osmoregulation facilitated by leaf structural and functional traits in Malabar nut (*Justicia Adhatoda* L.) along elevation gradient. *Pak J. Bot.* **56**, 1419–1429 (2024).
46. Travlos, I. & Chachalis, D. Drought adaptation strategies of weed and other neglected plants of arid environments. *Plant. Stress.* **2**, 40–44 (2008).
47. Bayat, H., Nemati, H., Tehranifar, A. & Gazanchian, A. Screening different crested wheatgrass (*Agropyron cristatum* (L.) Gaertner.) accessions for drought stress tolerance. *Archives Agro Soil. Sci.* **62**, 769–780 (2016).
48. Atif Riaz, A. R. et al. Effect of drought stress on growth and flowering of marigold (*Tagetes erecta* L.). (2013).
49. Mustafa, G. et al. Pretreatment with Chitosan arbitrates physiological processes and antioxidant defense system to increase drought tolerance in alfalfa (*Medicago sativa* L.). *J. Soil. Sci. Plant. Nutri.* **22**, 2169–2186 (2022).
50. Kaleem, M. et al. Role of leaf micro-structural modifications in modulation of growth and photosynthetic performance of aquatic halophyte *Fimbristylis complanata* (Retz.) under Temporal salinity regimes. *Sci. Rep.* **14**, 26442. <https://doi.org/10.1038/s41598-024-77589-y> (2024).
51. Sun, Y., Wang, Y., Deng, L., Shi, X. & Bai, X. Moderate soil salinity alleviates the impacts of drought on growth and water status of plants. *Rus J. Plant. Physiol.* **67**, 153–161 (2020).
52. Verbeke, S., Padilla-Díaz, C. M., Haesaert, G. & Steppe, K. Osmotic adjustment in wheat (*Triticum aestivum* L.) during pre-and post-anthesis drought. *Front. Plant. Sci.* **13**, 775652 (2022).
53. Saeidi, M. & Abdoli, M. Effect of drought stress during grain filling on yield and its components, gas exchange variables, and some physiological traits of wheat cultivars. *J. Agric. Sci. Technol.* **17**, 885–898 (2015).
54. Ahmad, Z. et al. Physiological responses of wheat to drought stress and its mitigation approaches. *Acta Physiol. Plant.* **40**, 1–13 (2018).
55. Iqbal, U. et al. Survival tactics of an endangered species *Withania coagulans* (Stocks) Dunal to arid environments. *Environ. Monit. Assess.* **195**, 1363 (2023).
56. Shoaib, M., Banerjee, B. P., Hayden, M. & Kant, S. Roots' drought adaptive traits in crop improvement. *Plants* **11**, 2256 (2022).
57. Shafiqat, W. et al. Effect of three water regimes on the physiological and anatomical structure of stem and leaves of different citrus rootstocks with distinct degrees of tolerance to drought stress. *Horticulturae* **7**, 554 (2021).
58. Iqbal, U., Hameed, M., Ahmad, F., Aqeel Ahmad, M. S. & Ashraf, M. Adaptive strategies for ecological fitness in *Calotropis procera* (Aiton) WT Aiton. *Arid Land. Res. Manage.* **36**, 197–223 (2022).

59. Iqbal, U. et al. Surviving the desert's grasp: decipherment phreatophyte *Tamarix aphylla* (L.) karst. Adaptive strategies for arid resilience. *Plant. Sci.* **347**, 112201 (2024).
60. Naeem, Z., Ahmad, M. S. A., Hameed, M. & Rasul, F. Physiological and anatomical modifications of *datura stramonium* L. roots collected from dry environments. *Pak J. Bot.* **55**, 1429–1438 (2023).
61. Irshad, M. et al. Elevation-driven modifications in tissue architecture and physiobiochemical traits of *Panicum antidotale* retz. In the Pothohar plateau, Pakistan. *Plant. Stress.* **11**, 100430 (2024).
62. SADI, B. et al. Desert blooms: unraveling palyno-anatomical diversity in arid boraginaceous taxa. *Pak J. Bot.* **56**, 1929–1944 (2024).
63. Bibi, S., Ahmad, M. S. A., Hameed, M. & Alvi, A. K. Modulation of physiological plasticity through structural and functional modifications in *Stipagrostis Plumosa* L. for adaptability to hyper-arid environments. *Turk. J. Bot.* **46**, 435–458 (2022).
64. Ahmad, I. et al. Morpho-anatomical determinants of yield potential in *Olea europaea* L. cultivars belonging to diversified origin grown in semi-arid environments. *Plos One.* **18**, e0286736 (2023).
65. Kaleem, M. et al. Role of leaf micro-structural modifications in modulation of growth and photosynthetic performance of aquatic halophyte *Fimbristylis complanata* (Retz.) under Temporal salinity regimes. *Sci. Rep.* **14**, 26442 (2024).
66. Basharat, S. et al. Structural and functional strategies in *Cenchrus* species to combat environmental extremities imposed by multiple abiotic stresses. *Plants* **13**, 203 (2024).
67. Iqbal, U., Hameed, M. & Ahmad, F. Water conservation strategies through anatomical traits in the endangered arid zone species *Salvadora Oleoides* decne. *Turk. J. Bot.* **45**, 140–157 (2021).
68. Fatima, S., Hameed, M., Ahmad, F., Ashraf, M. & Ahmad, R. Structural and functional modifications in a typical arid zone species *Aristida adscensionis* L. along altitudinal gradient. *Flora* **249**, 172–182 (2018).
69. Mansoor, U. et al. Structural modifications for drought tolerance in stem and leaves of *Cenchrus ciliaris* L. ecotypes from the Cholistan desert. *Flora* **261**, 151485 (2019).
70. Ahmad, K. S. et al. Morpho-anatomical and physiological adaptations to high altitude in some avenae grasses from neelum valley, Western Himalayan Kashmir. *Acta Physiol. Plant.* **38**, 93 (2016).
71. Drake, P. L., Froend, R. H. & Franks, P. J. Smaller, faster stomata: scaling of stomatal size, rate of response, and stomatal conductance. *J. Exp. Bot.* **64**, 495–505. <https://doi.org/10.1093/jxb/ers347> (2013).

## Acknowledgements

The authors extend their appreciation to the Deanship of Scientific Research, King Saud University for funding through the Vice Deanship of Scientific Research Chairs; Research Chair of Prince Sultan Bin Abdulaziz International Prize for Water.

## Author contributions

Conceptualization: U.I.; Supervision: UI, K.S.A., methodology, data collection, and original data analysis: S.R., S.A., M.M., A.M.; data presentation, writing: U.I., M.S., A.W.; reviewing and editing: U.I., K.S.A., S.S., E.A.M., and H.O.S.; funding acquisition: K.F.A., H.O.E. All authors have read and agreed to the published version of the manuscript.

## Funding

This research was funded by the Deanship of Scientific Research, King Saud University through the Vice Deanship of Scientific Research Chairs; Research Chair of Prince Sultan Bin Abdulaziz International Prize for Water.

## Declarations

## Competing interests

The authors declare no competing interests.

## Additional information

**Correspondence** and requests for materials should be addressed to K.S.A.

**Reprints and permissions information** is available at [www.nature.com/reprints](http://www.nature.com/reprints).

**Publisher's note** Springer Nature remains neutral with regard to jurisdictional claims in published maps and institutional affiliations.

**Open Access** This article is licensed under a Creative Commons Attribution-NonCommercial-NoDerivatives 4.0 International License, which permits any non-commercial use, sharing, distribution and reproduction in any medium or format, as long as you give appropriate credit to the original author(s) and the source, provide a link to the Creative Commons licence, and indicate if you modified the licensed material. You do not have permission under this licence to share adapted material derived from this article or parts of it. The images or other third party material in this article are included in the article's Creative Commons licence, unless indicated otherwise in a credit line to the material. If material is not included in the article's Creative Commons licence and your intended use is not permitted by statutory regulation or exceeds the permitted use, you will need to obtain permission directly from the copyright holder. To view a copy of this licence, visit <http://creativecommons.org/licenses/by-nc-nd/4.0/>.

© The Author(s) 2025